Molecular Plant Pathology

MOLECULAR PLANT PATHOLOGY (2016) 17(6), 903–919 DOI: 10.1111/mpp.12336

Skp1, a component of E3 ubiquitin ligase, is necessary for growth, sporulation, development and pathogenicity in rice blast fungus (*Magnaporthe oryzae*)

CHANDRA PRAKASH[1,2], JOHANNES MANJREKAR[1] AND BHARAT B. CHATTOO[1,2,*]

[1]*Department of Microbiology and Biotechnology Centre, The Maharaja Sayajirao University of Baroda, Vadodara 390 002, Gujarat, India*
[2]*Genome Research Centre, Faculty of Science, The Maharaja Sayajirao University of Baroda, Vadodara 390 002, Gujarat, India*

SUMMARY

Ubiqitination is an important process in eukaryotic cells involving E3 ubiquitin ligase, which co-ordinates with cell cycle proteins and controls various cell functions. Skp1 (S-phase kinase-associated protein 1) is a core component of the SCF (Skp1-Cullin 1-F-box) E3 ubiquitin ligase complex necessary for protein degradation by the 26S proteasomal pathway. The rice blast fungus *Magnaporthe oryzae* has a single *MoSKP1*(MGG_04978) required for viability. Skp1 has multiple functions; however, its roles in growth, sporulation and appressorial development are not understood. *MoSKP1* complements Skp1 function in the fission yeast temperature-sensitive mutant skp1 A7, restoring the normal length of yeast cells at restrictive temperature. The MoSkp1 protein in *M. oryzae* is present in spores and germ tubes, and is abundantly expressed in appressoria. Various RNA interference (RNAi) and antisense transformants of *MoSKP1* in B157 show reduced sporulation, defective spore morphology, lesser septation and diffuse nuclei. Further, they show elongated germ tubes and are unable to form appressoria. Transformants arrested in G1/S stage during initial spore germination show a similar phenotype to wild-type spores treated with hydroxyurea (HU). Reduced MoSkp1 transcript and protein levels in knock-down transformants result in atypical germ tube development. MoSkp1 interacts with the putative F-box protein (MGG_06351) revealing the ability to form protein complexes. Our investigation of the role of *MoSKP1* suggests that a decrease in MoSkp1 manifests in decreased total protein ubiquitination and, consequently, defective cell cycle and appressorial development. Thus, *MoSKP1* plays important roles in growth, sporulation, appressorial development and pathogenicity of *M. oryzae*.

Keywords: appressoria, cell cycle, conidiogenesis, E3 ubiquitin ligase, *Magnaporthe oryzae*, pathogenesis, Skp1-Cullin 1-F-box (SCF).

* *Correspondence*: Email: bharat.chattoo@bcmsu.ac.in

INTRODUCTION

Rice blast disease is one of the most devastating and recurring problems affecting rice production worldwide (Skamnioti and Gurr, 2009). The causal organism of rice blast is the ascomycetous fungus *Magnaporthe oryzae* (anamorph *Pyricularia grisea* Sacc), which infects rice and other grasses by producing a dome-shaped infection structure, known as an appressorium. The infection process starts when a three-celled conidium lands on the leaf surface and adheres to the surface by an adhesive released from the apex of the conidium; 60–90 min after attachment, the apical cell of the conidium gives rise to a polarized germ tube. Induction by a set of cues, including surface hardness, hydrophobicity, cuticular wax and the absence of exogenous nutrients, gives rise to the development of an appressorium (Ebbole, 2007; Gilbert *et al.*, 2006; Talbot, 2003; Wang *et al.*, 2005). Cell cycle and various signalling pathways govern the progression of appressorium development in *M. oryzae* during leaf infection. Mitosis is a prerequisite for appressorium development (Fourrey *et al.*, 2006), and appressorium-mediated plant infection is coordinated by three distinct cell cycle checkpoints (Saunders et al., 2010a, b). The morphogenesis of appressoria in *M. oryzae* is tightly regulated by the cell cycle, cyclic adenosine monophosphate (cAMP) and protein kinase A (Adachi and Hamer, 1998; Choi and Dean, 1997; Thines *et al.*, 2000; Xu and Hamer, 1996). The involvement of a G-protein-coupled receptor, Pth11, and cognate G-α- and G-$\beta\gamma$-subunit proteins has been reported in appressorial development (Wilson and Talbot, 2009). A mitogen-activated protein (MAP) kinase pathway composed of the Mst11, Mst7 and Pmk1 proteins is also essential for appressorium formation and subsequent invasive growth (Park *et al.*, 2006; Zhao and Xu, 2007; Zhao *et al.*, 2005, 2007). Previous work from our laboratory has demonstrated the involvement of MGA1 in appressorial development by changing the glycogen and lipid content of the germ tube (Gupta and Chattoo, 2007).

Reversible phosphorylation of cyclin-dependent kinases (Cdks) regulates various processes, such as DNA repair (Ariza *et al.*, 1996), protein–protein interactions and chromosome condensation (Siino *et al.*, 2003), but not the directionality of the cell cycle. The directionality is determined by the degradation of proteins that are needed in the previous stage of the cell cycle, making it irreversible and driving the cell cycle forward (Vodermaier, 2004).

Although cyclins are the activating units of Cdks, the destruction is mainly controlled by a proteasome system in which the substrate is recognized and tagged with ubiquitin by the E3 ubiquitin ligase enzyme, and subsequently degraded by the 26S proteasome (Murray, 2004; Renski *et al.*, 2008; Yu, 2007). The proteolysis is mainly carried out by the anaphase-promoting complex (APC/C) and the Skp1-Cullin 1-F-box (SCF) protein complex. Proteolytic control of cell cycle regulatory proteins is an important level of regulation of the cell cycle.

In the SCF complex of budding yeast, Skp1 (S-phase kinase-associated protein 1) associates with the Roc1-Cul1 heterodimer and bridges it to the substrate adaptor by virtue of its ability to interact with F-boxes. F-box-containing proteins bear additional protein–protein interaction motifs, such as WD40 repeats and leucine-rich repeats (LRRs), which recognize sequences in the target protein, which is the signal for destruction. Skp1 interacts with a variety of F-box proteins, suggesting a large range of potential substrates. For example, in budding yeast, SCF containing Cdc4 ($SCF1^{cdc4}$) ubiquitinates Sic1, Far1 and Cdc6; in addition, $SCF1^{\beta\text{-}TrCP}$ targets β-catenin or IκBα (Feldman *et al.*, 1997; Hattori *et al.*, 2003; Vodermaier, 2004; Yam *et al.*, 1999). Skp1 also has various functions other than the stabilization of the SCF complex. Skp1 has been reported to be associated with a protein complex, RAVE, required for vacuolar-type H^+-ATPase (V-ATPase) assembly. V-ATPases are conserved throughout eukaryotes and have been implicated in metastasis and multidrug resistance (Seol *et al.*, 2001). Skp1 has also been reported to interact with Rav1p, which is not involved in V-ATPase assembly, but in recycling of the complex (Brace *et al.*, 2006). In fission yeast, Skp1 interacts with the Pof-6 protein and is essential for cell separation (Hermand *et al.*, 2003), as well as spindle morphology and nuclear membrane segregation in anaphase (Lehmann and Toda, 2004). Recent reports have shown that E3 ubiquitin ligase-mediated protein degradation is involved in plant–pathogen interactions. *Pseudomonas syringae* gains access by targeting the host protein and making the host plant susceptible (Rosebrock *et al.*, 2007), and *Xanthomonas campestris* hijacks the host ubiquitination machinery (Singer *et al.*, 2013). The Skp1 of *Arabidopsis* interacts with F-box domain-containing effectors of the type 3 secretion systems (T3SS) of the phytopathogenic bacterium *Ralstonia solanacearum* and facilitates the development of disease in the host (Angot *et al.*, 2006). It appears that Skp1 is a vital element with varied functions based on the protein partners with which it interacts under various physiological conditions and at diverse locations in each host system.

In *Schizosaccharomyces pombe*, *skp1* mutants have been shown to affect mitosis; specifically, mutants fail to proceed to anaphase and show growth retardation (Lehmann and Toda, 2004, Lehmann *et al.*, 2004). In our study, with the same mutant background of fission yeast, interspecies gene complementation by *MoSKP1* showed restoration of normal phenotypes, such as cell size and shape, septation patterns and nuclear organization.

Our analysis of the *M. oryzae* genome data suggests the presence of only one orthologue of *skp1*. Here, we have shown that MoSkp1 is important for cell cycle progression and growth, sporulation, cell wall integrity, cell septation, nuclear organization, development of appressoria and pathogenicity in *M. oryzae* B157.

RESULTS

Features of *MoSKP1* gene and protein

Based on the yeast *SKP1* coding region, the *MoSKP1* open reading frame (ORF) was identified from the Genomic Resources of *Magnaporthe oryzae* (GROMO, http://gromo.msubiotech.ac.in/Gromo/home.htm) (Thakur *et al.*, 2009). Genes involved in the SCF complex assembly were analysed and it was observed that a single *SKP1* orthologue was present in the *M. oryzae* genome. The Broad Institute database revealed that *MoSKP1* was located on the minus strand of the DNA and had two introns. Sequence information on the *MoSKP1* coding region was obtained from an earlier version of annotation (MGG_04978.5) in order to amplify a 645-bp ORF. Subsequently, cDNA was synthesized and cloned in the bacterial expression vector pET30a, and MoSkp1 protein was expressed. Using an updated version of annotation of *MoSKP1* (MGG_04978.6) released by the Broad Institute showing a total of 793 bp, a National Center for Biotechnology Information (NCBI) BLASTP search was performed taking MoSkp1 as a query sequence, and 30 homologous sequences with more than 90% coverage information were obtained to generate a phylogenetic tree. The molecular phylogenetic analysis by maximum likelihood method, performed using MEGA version 5.10 (Jones *et al.*, 1992; Tamura *et al.*, 2011), indicated that the *Neurospora crassa* Skp1 (AY673971) is the closest match to MoSkp1 with a branch length of 0.0222 and highest likelihood coefficient (−3093.0536) (Fig.1a). Multiple sequence alignment was carried out including sequences from *Fusarium oxysporum*, *N. crassa*, *Sc. pombe*, *Saccharomyces cerevisiae* and human to evaluate the conservation of the Skp1 protein among eukaryotes. A high level of sequence similarity was found with *F. oxysporum* (identity 81% at the protein level with 100% query coverage), *Sc. pombe* Skp1 (identity 70% at the protein level with 97% query coverage), *S. cerevisiae* Cbf3d protein (identity 56% at the protein level with 95% query coverage) and human Skp1 (identity 57% at the protein level with 95% query coverage). Multiple sequence alignment revealed that the C-terminal region was most highly conserved among these Skp1 proteins. Skp1 shows affinity to a subset of F-box proteins, which is a characteristic feature of the family. On the basis of the crystal structure, human Skp1 has eight α-helices and three β-sheets, of which the H5, H6 and H7 helices present at the C-terminus are involved in binding with the H1, H2 and H3 helices and the L1

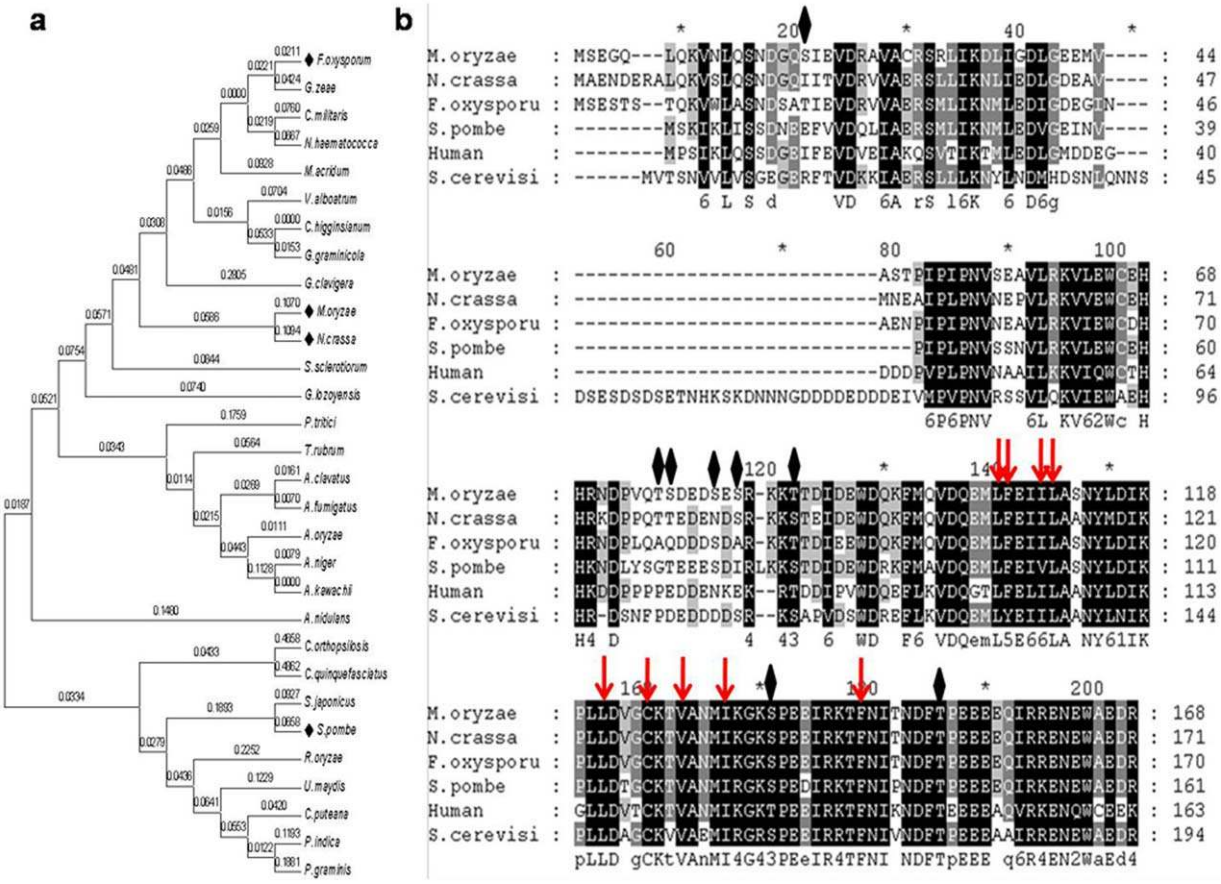

Fig. 1 Identification of MoSkp1 in *Magnaporthe oryzae*. (a) Evolutionary history was inferred using the maximum likelihood method. The tree with the highest log likelihood (−3093.0536) is shown. The analysis involved 30 amino acid sequences. Evolutionary analyses were conducted in MEGA5 (the list of strains used in the phylogenetic analysis is given in List S1, see Supporting Information). (b) Multiple sequence alignment of the amino acid sequence was performed using the CLUSTALX 2.0.11 tool. Arrows show the amino acids conserved among *M. oryzae*, *Neurospora crassa*, *Fusarium oxysporum*, *Schizosaccharomyces pombe*, human and *Saccharomyces cerevisiae*. Amino acids (Leu-105, Phe-106, Ile-109, Val-128 and Phe-144) and (Ile-109, Leu-110, Leu-121, Cys-125, Val-128 and Ile-132) are situated in the C-terminal region and are responsible for interaction with the L1 and H1 domains of the F-box protein, respectively. Black diamonds indicate putative phosphorylation sites at the amino acids (Ser-18, 77, 81, 83, 136) and (Thr-76, 87, 151) in the sequence. The distribution of phosphorylation sites in *M. oryzae* is clustered from amino acids 76 to 87.

loop at the N-terminus of F-box proteins (Schulman *et al.*, 2000). The multiple sequence alignment of MoSkp1 with human Skp1 revealed the conservation of amino acids leucine (Leu)-105, phenylalanine (Phe)-106, isoleucine (Ile)-109, Leu-110, valine (Val)-128 and Phe-144, which are involved in binding with the L1 loop of the F-box, and Ile-105, Leu-110, Leu-121, cysteine (Cys)-125, Val-128 and Ile-132, which bind with the H1 helix of the F-box proteins (Fig. 1b).

MoSKP1 complements the function of Skp1 in the *skp1 A7* mutant of *Sc. pombe* and shows conserved protein function in *M. oryzae* B157

As *M. oryzae* B157 *MoSKP1* knockout mutants are not viable (data not shown), a cross-species genetic complementation was carried out in *Sc. pombe* utilizing *MoSKP1*. An *skp1* temperature-sensitive (ts) mutant of *Sc. pombe*, s*kp1 A7*, shows G2 delay and a cell elongation phenotype (Hermand *et al.*, 2003; Lehmann *et al.*, 2004). The ts allele carries a point mutation at position T454C that results in amino acid substitution I110T. At the restrictive temperature of 37 °C, the s*kp1 A7* mutant remains in G2 phase, resulting in an elongated cell phenotype (Lehmann *et al.*, 2004). The G2 delay seen in these cells is a consequence of the activation of a DNA damage checkpoint, and this phenotype can be rescued by inactivation of the checkpoint.

The s*kp1 A7* mutant strain was transformed with a pYES2-*MoSKP1* construct, and the ability of the recombinant *Sc. pombe* pYES2-*MoSKP1 skp1 A7* to grow on medium lacking uracil was tested. The recombinant strain grew on Edinburgh minimal medium (EMM) without uracil, in contrast with the non-recombinant s*kp1 A7*

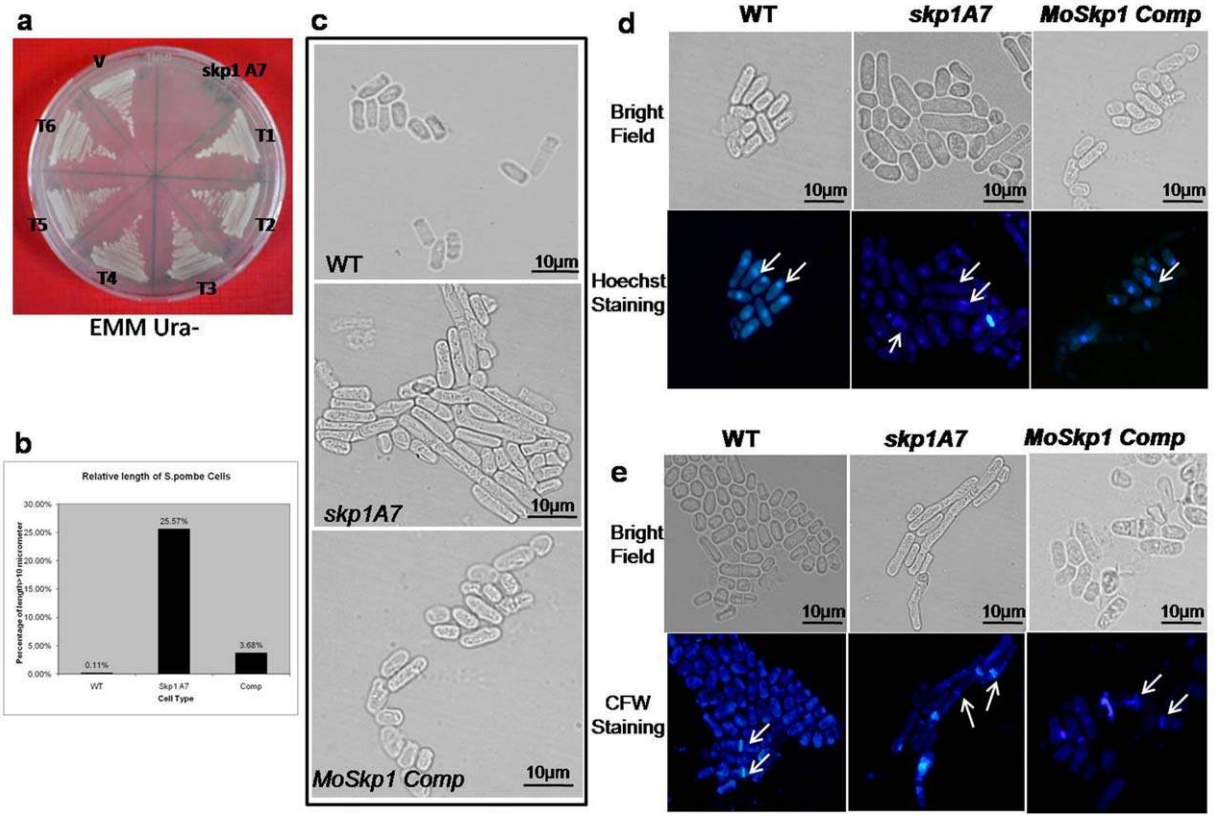

Fig. 2 MoSkp1 is able to complement the function of *Schizosaccharomyces pombe skp1 A7* mutation and rescue nuclear disorganization and multiple septation. (a) *Schizosaccharomyces pombe skp1 A7* strain was transformed with pYES2-*MoSKP1* expression vector and pYES2 empty vector and selected on Edinburgh minimal medium (EMM) agar without uracil. (b) Cells were grown at 25 °C and then transferred to 37 °C for 4 h, and the length of *Sc. pombe MoSKP1*-transformed and *skp1 A7* cells was observed under a microscope. For each strain, 100 cells were counted and the percentage of cells with elongated phenotype was calculated. The experiment was performed in triplicate and the level of significance was calculated at 5% *P* value. (c) Micrographs of wild-type (WT), *skp1 A7* mutant and complemented strain were taken at 100× magnification. (d) Nuclear staining was performed using Hoechst 3342 stain to visualize the nuclear organization. Cells were grown in EMM broth at 25 °C and transferred to 37 °C for 4 h; 50 μL of cell suspension was fixed and stained for 10 min, and observed using fluorescence microscopy. (e) The septum of *Sc. pombe* was stained with calcofluor white (CFW) stain. Cells were induced at restrictive temperature. Around 200 cells were counted for each strain and the percentage of multiseptate cells was determined.

mutant (Fig. 2a). The strain with empty vector pYES2 grew on selection medium, but was unable to rescue the phenotype of the *Sc. pombe skp1 A7* mutant. The average length of the *skp1 A7* mutant cells was 23 μm, which was restored to a normal length of around 10 μm (similar to that of wild-type cells) in the complemented strain (Fig. 2b,c). The *skp1 A7* mutant transformed with pYES2-*MoSKP1* was grown with and without 2% galactose (GAL1 promoter active in the presence of galactose), and nuclear status was evaluated by staining with Hoechst 3342 stain. As expected, the 'cut' phenotype and septation without chromosome segregation (indicative of a cell cycle defect) of the s*kp1 A7* mutant were rescued, together with the elongated cell phenotype, at restrictive temperature (Fig. 2d). Calcofluor white (CFW) staining of the s*kp1 A7* mutant showed aberrant septum formation and defective cell separation, whereas there was restoration of normal septation in the complemented strain at the restrictive temperature of 37 °C (Fig. 2e), indicating that the *MoSKP1* gene has functions similar to its counterpart in fission yeast. It can be concluded that *MoSKP1* retained its essential function at restrictive temperature (37 °C), although the complemented strain showed delayed growth, with colonies being noticeably smaller on the fifth day relative to the *Sc. pombe skp1* A7 mutant strain, probably because of overexpression of the *MoSKP1* gene.

Localization of MoSkp1 in *M. oryzae* B157

Skp1 is a cytosolic protein in *S. cerevisiae* (Seol *et al.*, 2001). The *in vivo* localization of the MoSkp1 protein in *M. oryzae* B157 provides significant information on the physiological role of this protein. Immunolocalization was carried out in wild-type *M. oryzae* B157 strain with a 20-μL spore suspension (1×10^4 spore/mL) spread on a coverslip, which was allowed to grow for 8 h under moist conditions at 28 °C. Polyclonal primary antibody against

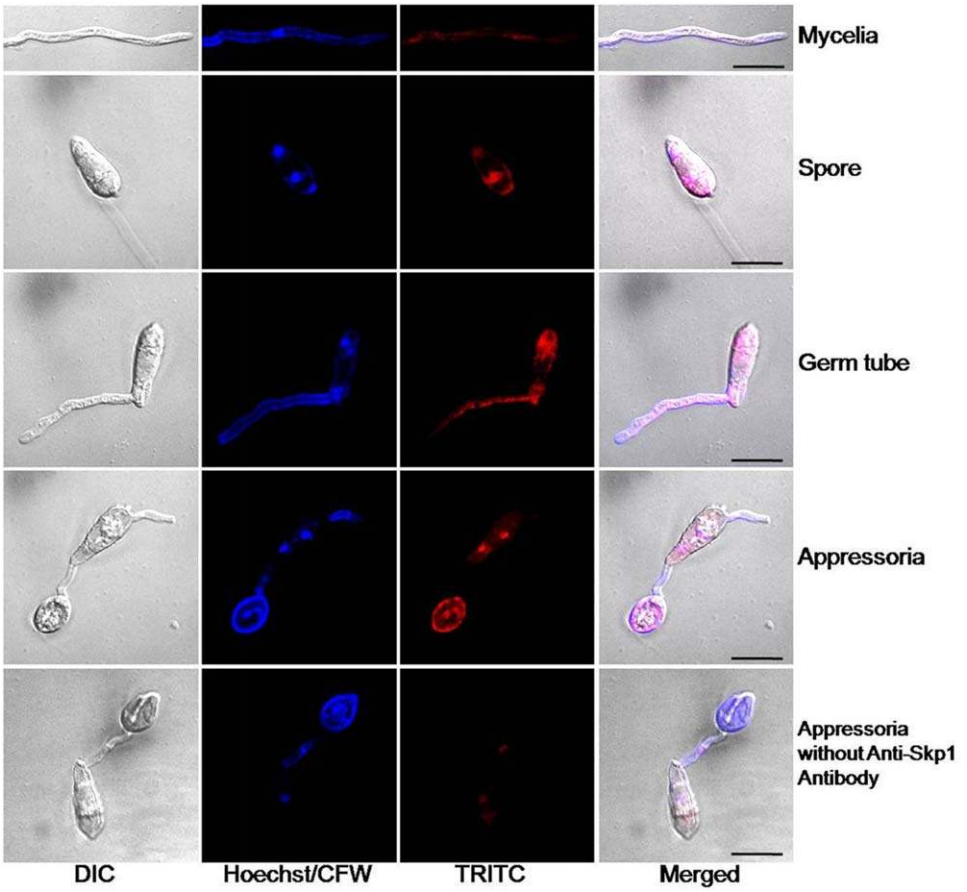

Fig. 3 Subcellular localization of MoSkp1 protein in *Magnaporthe oryzae* B157. MoSkp1 localization was studied in mycelia, spores, germ tubes and appressoria by immunostaining using anti-Skp1 antibody and tetramethyl rhodamine isothiocyanate (TRITC)-conjugated secondary antibody. Appressoria staining without anti-Skp1 antibody was used as a negative control. In the spore, MoSkp1 localizes in the cytoplasm. As the spore germinates, MoSkp1 is enriched in the germ tube and appressoria. Calcofluor white (CFW) and Hoechst 3342 stain were used to stain chitin and nucleus, respectively. Differential interference contrast (DIC). Bar, 10 μm.

MoSkp1 protein generated in rabbit and commercially obtained secondary antibody conjugated with tetramethyl rhodamine isothiocyanate (TRITC) were used for localization. MoSkp1 was found to be localized in the cytoplasm of spores, germ tube and mature appressorium. CFW staining did not show any association of MoSkp1 with the membrane (Fig. 3). The level of MoSkp1 protein increased from spores to appressoria and gradually diminished to a basal level in hyphae, suggesting the accumulation of MoSkp1 in dividing cells. The real-time polymerase chain reaction (PCR) data from spores, germ tube and appressoria suggested that the *MoSKP1* transcript level was six-fold higher in appressoria when compared with mycelia. The transcripts were below detectable levels in the spores and germ tube 4 h after germination, but, by 6 h after spore germination, *MoSKP1* transcripts were detectable (Fig. S6a, see Supporting Information).

Silencing of *MoSKP1* results in delayed germination, reduced sporulation, an elongated germ tube and the inability to form appressoria

For subsequent genetic and phenotypic analysis of MoSkp1, two sets of *MoSKP1*-silenced knockdown transformants were generated: RNA interference (RNAi) and antisense. Initially, an attempt was made to disrupt *MoSKP1*, but no true *MoSKP1* disruptants could be obtained using pGKO2-MoSkp1 dual selection vector following *Agrobacterium tumefaciens*-mediated transformation (data not shown). *MoSKP1* is likely to be essential for the viability of *M. oryzae* B157, as is the case with yeast (Stemmann and Lechner, 1996). In two RNAi and antisense transformants, integration of vector DNA was confirmed by Southern blot analysis, and silencing was verified by Western blot (Fig. S1, see Supporting Information). The growth rate of *MoSKP1* RNAi transformants was found to be slower than that of the wild-type B157 strain. Similar observations from *MoSKP1* antisense transformants confirmed the role of Skp1 in growth. Sporulation was reduced and delayed in the case of the *MoSKP1* RNAi transformants, indicating that a reduced level of MoSkp1 protein leads to delayed cell division and/or defects in the cell division cycle. This result was consistent with the reduced transcript levels in the *MoSKP1* RNAi transformants when checked by quantitative real-time PCR using SYBR Green chemistry. Transcript level evaluation of *MoSKP1* in RNAi and antisense transformants confirmed that RNAi transformants had lower transcript levels (~15% to ~40%), whereas antisense transformants had comparatively higher *MoSKP1*

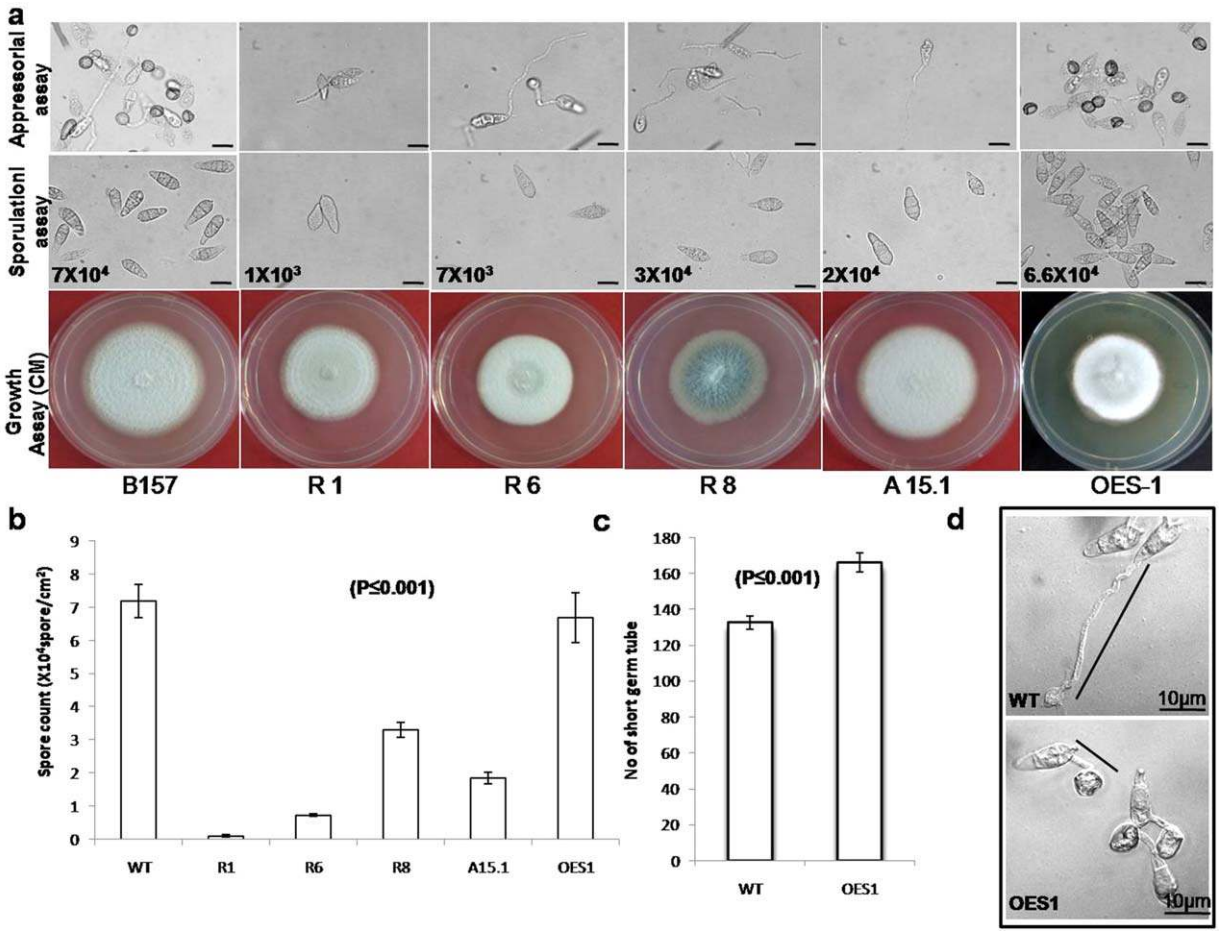

Fig. 4 Growth, sporulation and appressorial assay of *MoSKP1* transformants. (a) Growth of the transformants was checked on complete medium (CM) for 7 days. Sporulation was checked at 8 days post-inoculation on oat meal agar (OMA) and the ability to form appressoria was assayed on a hydrophobic coverglass. (b) The sporulation efficiency of transformants was quantified ($P < 0.001$). (c) The length of the germ tube between spore and appressorium was measured in the overexpression transformant OES1 and compared with B157. Two hundred appressoria were counted and the difference between the number of smaller germ tubes (≤ 25 μm) between OES1 and B157 was calculated to be significant ($P < 0.001$). (d) Micrograph showing the length of the germ tube in transformant OES1 and the B157 strain. Bar, 10 μm.

transcript levels (~40% to ~60%) (Fig. S2, see Supporting Information). Five *MoSKP1* RNAi transformants which showed *MoSKP1* transcript levels in the range 15%–40% were analysed further. Two *MoSKP1* RNAi transformants (R1 and R2) sporulated only on the 10th day after inoculation. Spore numbers were in the region of 1×10^3 spores/cm^2, in contrast with wild-type B157, which showed 7×10^4 spores/cm^2. The other three *MoSKP1* RNAi transformants (R3, R6 and R8) were able to sporulate on the eighth day, with around 3.3×10^4 spores/cm^2. The spore count was adjusted to 1×10^4 spores/mL and appressorial assay was performed in order to examine the further development of spores on a hydrophobic glass coverslip (Fig. 4a, Table 1). Most of the spores were unable to germinate until 12 h in transformant R1, whereas R6 and R8, which germinated, showed elongated germ tubes, but did not develop appressoria. Elongated germ tubes were also observed in a few of the antisense transformants, such as A15.1 and A6. Germination studies up to 36 h showed the absence of hook structure formation and occasional branching of the germ tube (A2, A3, A15.1). None of the antisense transformants showed an inability to sporulate. Microscopic examination of conidia on conidiophores showed that R1 and R6 showed reduced and abnormal sporulation (Fig. 5a). It appears that the differences in sporulation, spore germination and length of the germ tube are correlated with differences in the levels of *MoSKP1* silencing in the various RNAi and antisense transformants.

MoSKP1 overexpression enhances appressoria development

The wild-type B157 strain was transformed with an overexpression construct of *MoSKP1* and the transformants were checked for

Table 1 Comparison of mycological characteristics among various transformants.

Strain	Mycelial growth* (mm)	Conidiation† (10^4/cm^2)	Conidial germination‡ (%)	Double septa conidia§ (%)	Conidia with single septum§ (%)	No septa conidia§ (%)	Appressorium formation¶ (%)
Wild-type	66 ± 1.41	7.18 ± 0.49	90.33 ± 4.50	88 ± 2.64	8 ± 2	4.66 ± 0.57	86.33 ± 5.13
RNAi 1	41.5 ± 2.12	0.10 ± 0.04	34 ± 5.29	44.66 ± 4.50	29 ± 1	25.66 ± 3.78	7 ± 4.35
RNAi 6	40 ± 1.41	0.73 ± 0.03	44.66 ± 5.03	59 ± 1	29.33 ± 1.15	11.66 ± 2.08	6 ± 3.6
RNAi 8	43.5 ± 2.12	3.30 ± 0.22	61 ± 1	70.33 ± 1.52	24 ± 3.60	5.66 ± 2.51	11 ± 1.73
A 15.1	51 ± 1.41	1.85 ± 0.17	88.66 ± 3.21	77.66 ± 2.51	20 ± 1	2.33 ± 2.30	4.33 ± 1.15
OES1	66.5 ± 0.70	6.69 ± 0.74	96.33 ± 0.57	94 ± 1	4 ± 1	4.66 ± 1.52	96.66 ± 1.52

Statistical analysis was performed using analysis of variance (ANOVA) with $P \leq 0.001$ as a significant value.

*Growth was measured as the diameter (mm) of mycelium 7 days after inoculation.

†Conidiation assay was performed by isolating conidia in 1 mL of sterile water from the same plate as used for growth measurement, and values are represented as the number of spores per square centimetre.

‡Germination ability was measured as the ratio of germinating conidia to total conidia.

§Septation was counted after staining with calcofluor white (CFW). Of 100 conidia, conidia with double septa, single septa and without septa were counted.

¶Appressorium formation was measured as the ratio of appressorium-forming conidia to germinating conidia on a hydrophobic coverglass.

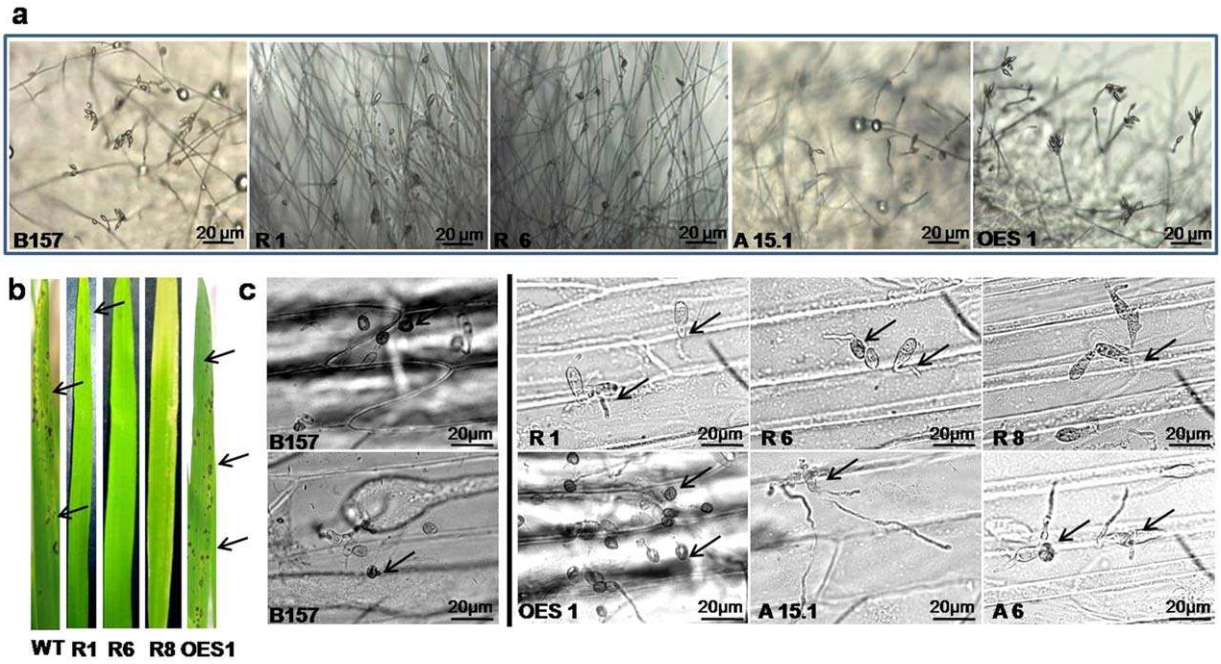

Fig. 5 Abnormal conidia production in *MoSKP*1 RNAi transformants and inability to infect rice leaves and penetrate onion epidermis. (a) Microscopic examination of number of conidia on conidiophores. (b) Spore count was maintained at 1×10^4/ml for each transformants and spray inoculation method was applied to 21 days old leaf of CO-39 rice line. After seven days, the severity of infection was measured. (c) Onion epidermis assay was performed taking *MoSKP*1 RNAi, antisense and overexpression OES1 transformants. After 12 h of inoculation samples were observed under microscope at 100× magnification.

growth, sporulation and appressorial development. The transcript level of *MoSKP1* in the overexpression transformant (OES1) was 2.4-fold higher, and growth and sporulation were comparable, with that of the B157 strain on complete medium (CM) (Fig. 4a,b). The efficiency of appressoria formation in the OES1 transformant was increased compared with that of the wild-type B157 strain. It was observed that the length of the germ tube between conidia and appressoria was reduced in OES1 which developed appressoria. Approximately 80% of germ tubes were 15 µm or less in OES1, whereas, in the wild-type B157 strain, only ~30% appressoria showed shorter germ tubes (Fig. 4c,d).

MoSKP1 RNAi transformants are unable to infect the plant host

Rice leaf infection assay of *MoSKP1* RNAi transformants was performed using standard protocols (Bonman, 1992; Bonman *et al.*, 1988). Leaves of 21-day-old CO39 (a dwarf cultivar susceptible to

M. oryzae) plants were inoculated using the spray inoculation method with a spore suspension of 1×10^5 spores/mL, and observed for 7 days under high humidity (90%) at 28 °C. No blast lesions were observed until 10 days post-inoculation (dpi) in *MoSKP1* RNAi transformants (R1, R6 and R8), whereas spindle-shaped lesions could be observed on leaves inoculated with spores of wild-type *M. oryzae* B157 strain and the OES1 *MoSKP1* overexpression strain. The development of blast lesions was quantified as the percentage disease leaf area (% DLA = disease leaf area × 100/total leaf area). Wild-type B157 *M. oryzae* and OES1 transformants showed up to 50% DLA, whereas knockdown transformants were hardly able to develop blast lesions (Figs 5b and S6b). In addition, it was observed that spores of these transformants were unable to germinate and penetrate onion epidermis. The RNAi transformant R8 grew on the leaf surface, but was unable to form appressoria; on onion epidermis too, it grew, but failed to develop appressoria (Fig. 5c). Thus, the level of 40% *MoSKP1* transcript (found in R8) is not sufficient for the development of appressoria and successful plant infection. Although the antisense transformant A15.1 had an *MoSKP1* transcript level of 60%, it was able to grow a germ tube, but was unable to form appressoria and penetrate host tissue.

MoSKP1 RNAi transformants are abnormal in septa formation and nuclear organization with defective cell walls

A previous study has shown that, during the development of appressoria, the nucleus of *M. oryzae* spores is degraded by non-selective macroautophagy. During infection, nuclear disorganization is the necessary event and indicator of autophagy in *M. oryzae* (He *et al.*, 2012). In order to investigate the effect of silencing in spores of *MoSKP1* RNAi transformants, we performed staining of septa and nuclei. CFW is a fluorescent stain that binds strongly with cellulose and chitin present in the fungal cell wall and septa. Staining revealed that the majority of spore septa of R1, R6 and R8 transformants were unstained, representing defective septa formation. Microscopy confirmed that the transformant spores showed reduced septa formation. Single septa formation was observed in 20%–25% of the total number of spores, whereas 25% of spores completely lacked septa formation in R1 transformants (Figs 6a and S3, see Supporting Information). This observation suggests that *MoSKP1* gene silencing might cause defective cell division and cytokinesis. The nuclear organization of these transformants was also examined by nuclear staining using Hoechst 3342 fluorescent dye. The nuclei were found to be diffuse relative to the wild-type (Fig. 6b). Studies on the s*kp1 A7* mutant of *Sc. pombe* have also indicated similar nuclear disorganization, a reflection of the defective cell division cycle in the yeast. Therefore, from the present study, it can be presumed that the *MoSKP1* RNAi transformants of *M. oryzae* B157 also show nuclear disorganization as a result of low levels of MoSkp1.

The cell wall integrity of the transformants was checked by growing them in the presence of the cell wall-disrupting agents caffeine (2.5 mM), Congo red (2 mg/mL) and CFW (200 mM). RNAi and antisense transformants were unable to grow on CFW and Congo red. In the presence of caffeine, growth was decreased relative to B157 and OES1 (Fig. 7, Table 2).

MoSKP1 RNAi transformants and antisense transformants are defective in cell division

Previous studies have shown that cellular differentiation, morphogenesis and the development of appressoria in *M. oryzae* are tightly regulated by mitosis and cytokinesis in the extending germ tube (Saunders *et al.*, 2010a, b). In order to compare the effect of cell cycle arrest and *MoSKP1* knockdown on development, the wild-type B157 strain of *M. oryzae* was treated with hydroxyurea (HU, 200 mM), a known inhibitor of cell cycle progression that functions by inhibiting DNA replication and activating the checkpoint at the G1/S phase (Koc *et al.*, 2004; Singer and Johnston, 1981). The wild-type B157 strain of *M. oryzae* was unable to form appressoria after treatment with HU and showed development of the germ tube comparable with that of the *MoSKP1*-RNAi antisense transformants of *M. oryzae* (Fig. 8). Fission yeast *skp1* mutants have been shown to arrest in either G1 or G2 of the cell cycle, which leads to elongated cells (Bai *et al.*, 1996; Connelly and Hieter, 1996; Kaplan *et al.*, 1997; Skowyra *et al.*, 1997). The defective septa, nuclear disorganization and elongated germ tube phenotype in silenced lines of *M. oryzae* clearly suggest cell cycle defects in the absence or at low levels of MoSkp1 protein.

MoSKP1 RNAi transformants are defective in total protein ubiquitination pattern compared with the wild-type B157 strain

The ubiquitin proteasome pathway is the principal mechanism for protein catabolism. This pathway is centrally involved in the regulation of a variety of cellular processes, including DNA repair, signal transduction, cell metabolism and growth (Oh *et al.*, 2012). Differences in total ubiquitination and in the ubiquitination of specific proteins affect numerous pathological conditions. As the MoSkp1 protein stabilizes the E3 ubiquitin ligase, ubiquitination enrichment assay was carried out to determine the ubiquitination profile in *M. oryzae* RNAi transformants. RNAi transformant R6 with 70% transcript reduction was selected, and total ubiquitinylated protein was enriched using an anti-ubiquitin affinity column. Western blot analysis was performed and ubiquitinylated proteins were detected with anti-ubiquitin antibody. Comparison of the ubiquitinylation pattern of total proteins in R6 RNAi transformants with that of wild-type *M. oryzae* B157 was performed, and a prominent decrease in the number of ubiquitinylated protein bands was

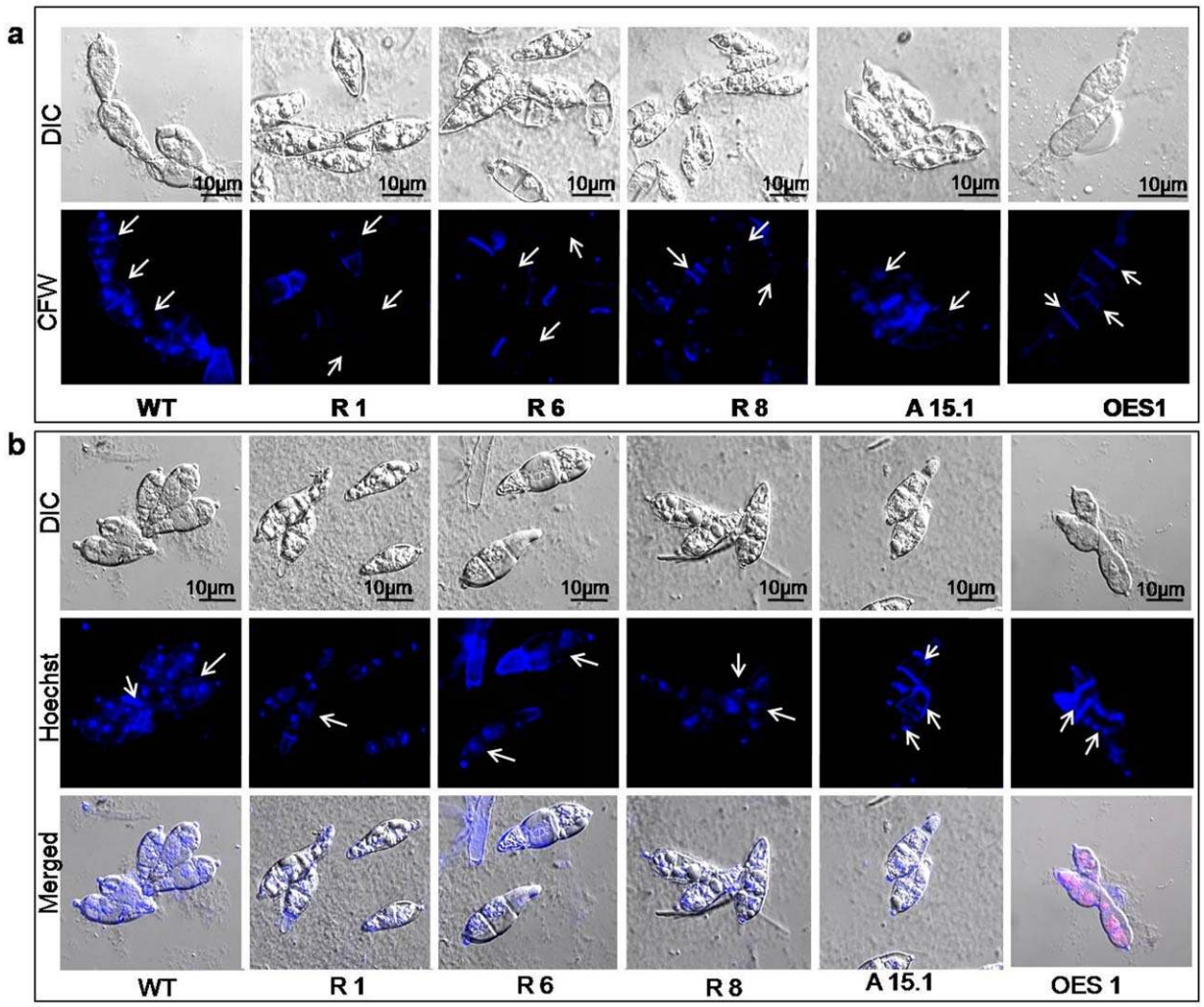

Fig. 6 Defective septation and nuclear disorganization in conidia of *MoSKP1* RNA interference (RNAi) and antisense transformants. (a) Calcofluor white (CFW) stain was used to stain chitin and conidial cell septa of various transformants. Arrows indicate the absence of septation in RNAi transformants. (b) Hoechst staining of *MoSKP1* knockdown transformants was performed to show the nuclear organization in the defective spores. Arrows indicate the diffused and disorganized nuclei in the transformants. Differential interference contrast (DIC).

observed in R6 (Fig. S4, see Supporting Information). The decrease in *MoSKP1* transcript level results in less MoSkp1 protein and therefore reduced ubiquitination of proteins. This further leads to various physiological conditions in silenced lines of *M. oryzae*. The decrease in MoSkp1 protein in *M. oryzae* leads to hindered development of appressoria, and the cumulative effect of various proteins with decreased ubiquitination is likely to have additional morphological, developmental and physiological effects.

MoSkp1 interacts with the F-box protein MoFrp1

In *Sc. pombe*, Skp1 is required for various functions, such as the activation of Ctf13 in the kinetochore, in the centromere-binding protein Cbf3 complex, in the recycling of SNARE and in the formation of the RAVE complex to promote the assembly of vacuolar ATPase holoenzyme, etc. (Seol *et al.*, 2001). Skp1 facilitates the above functions in association with various F-box proteins containing a WD motif or LRRs. In order to examine the ability of MoSkp1 to interact with F-box proteins, a yeast two-hybrid assay was performed using a putative interaction partner F-box protein MoFrp1 (MGG_06351). Sequence analysis of MoFrp1 showed an F-box domain at the N-terminus of the protein with a stretch of 50 amino acids having the LRR and WD40 protein–protein interaction domains. MoFrp1 was found to be a close homologue (53% identity at the protein level with 98% query coverage) of Frp1 from *F. oxysporum* (AY673970), required for pathogenesis in tomato (Duyvesteijn *et al.*, 2005). *Saccharomyces cerevisiae* cells (AH 109) were transformed using prey and bait vector containing

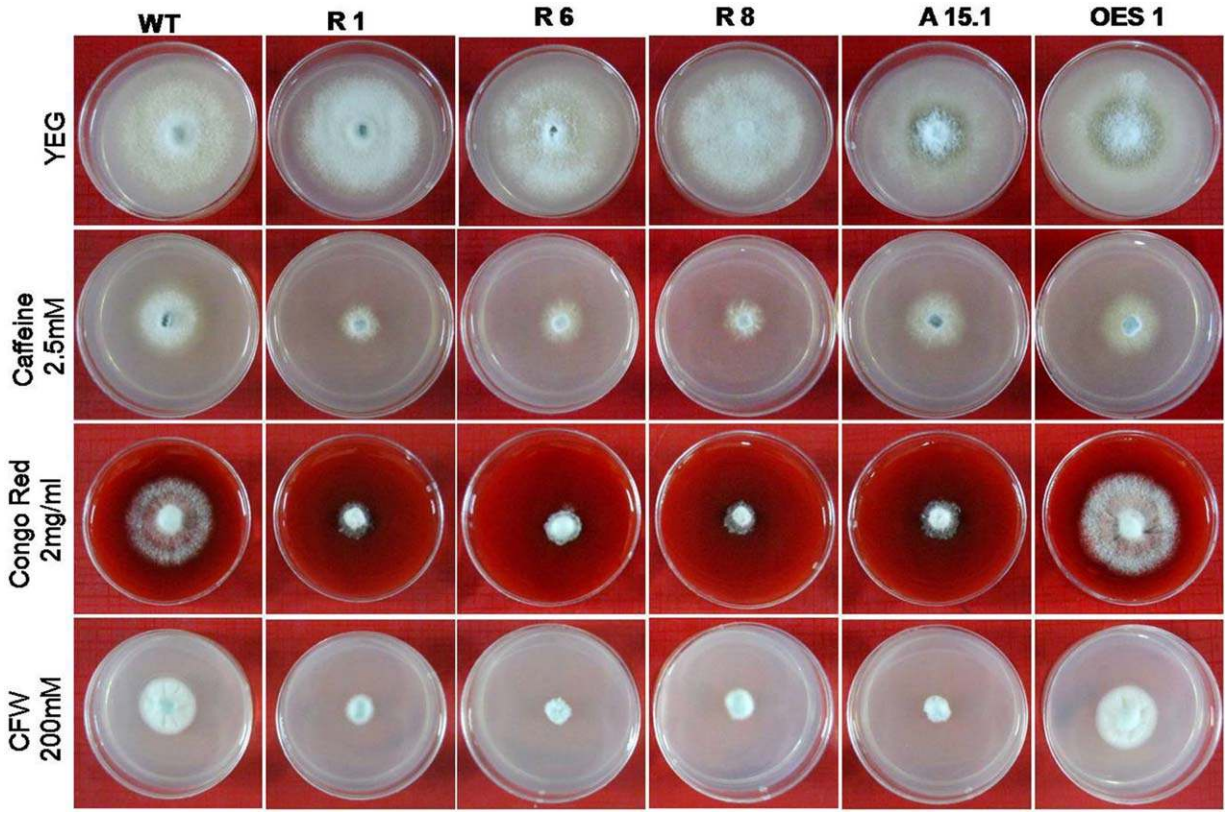

Fig. 7 *MoSKP1* RNA interference (RNAi) and antisense transformants are defective in cell wall integrity. The cell wall integrity of transformants was checked by growing on yeast extract glucose agar (YEG) medium containing caffeine (2.5 mM), Congo red (2 mg/mL) and calcofluor white (CFW) (200 mM). Inoculation was performed with a 2 mm × 2 mm mycelial plug for each culture and the diameter of growth was measured after 5 days. The experiments were performed in duplicate.

Table 2 Comparison of mycelial growth of transformants in the presence of cell wall-disrupting agents.

Strain	YEG (mm)	Caffeine (2.5 mM) (mm)	Congo red (2 mg/mL) (mm)	CFW (200 mM) (mm)
Wild-type	26 ± 1.41	12.5 ± 0.70	16 ± 1.41	9.5 ± 0.70
R1	27 ± 1.41	4.5 ± 0.70	3.5 ± 0.70	3.5 ± 0.70
R6	28.5 ± 0.70	3.5 ± 0.70	4 ± 1.41	3 ± 0.0
R8	28.5 ± 0.70	4.5 ± 0.70	4 ± 0.0	3.5 ± 0.70
A15.1	28 ± 0.0	6.5 ± 0.70	4 ± 1.41	3 ± 0.0
OES1	28 ± 0.0	7.5 ± 0.70	18 ± 0.0	11.5 ± 0.70

CFW, calcofluor white; YEG, yeast extract glucose agar.
Growth was measured as the diameter of mycelial growth 5 days after inoculation.

MoFRP1 and *MoSKP1*, respectively. The transformants were able to grow on quadruple dropout minimal medium (SD–Trp,–Leu,–His,–Ade), which is indicative of an interaction between the two proteins. The interaction was further confirmed by co-immunoprecipitation and pull-down (Fig. S5, see Supporting Information).

DISCUSSION

Targeted protein degradation by the ubiquitin proteasome pathway plays a pivotal role in monitoring most of the short-lived proteins in the cell, and thus controls many physiological conditions. Once the signal for the degradation of a particular protein is 'on', a cascade of three enzymes (E1, E2 and E3) acts on it and finally tags the protein with ubiquitin at an internal lysine residue of the substrate protein. This tagging is an important step carried out by a specialized protein, E3 ubiquitin ligase, which is a multiprotein complex (Skp1-Cullin 1-F-box) also known as SCF. Skp1 is the core protein of this complex and stabilizes the E3 ubiquitin ligase enzyme. Apart from its role in the SCF complex, Skp1 may have novel functions in mitotic exit and cytokinesis, in the regulation of the assembly of vacuolar ATPase, in connecting cell cycle regulation to the ubiquitin proteolysis machinery, in the DNA damage checkpoint and in the regulation of the kinetochore (Bai *et al.*, 1996; Brace *et al.*, 2006; Hermand *et al.*, 2003; Kaplan *et al.*, 1997; Kim *et al.*, 2006; Lehmann *et al.*, 2004). *Magnaporthe oryzae nim1* and *bim1* mutants show that cell cycle checkpoints regulate appressorium morphogenesis. Mutations of *nim1*, the

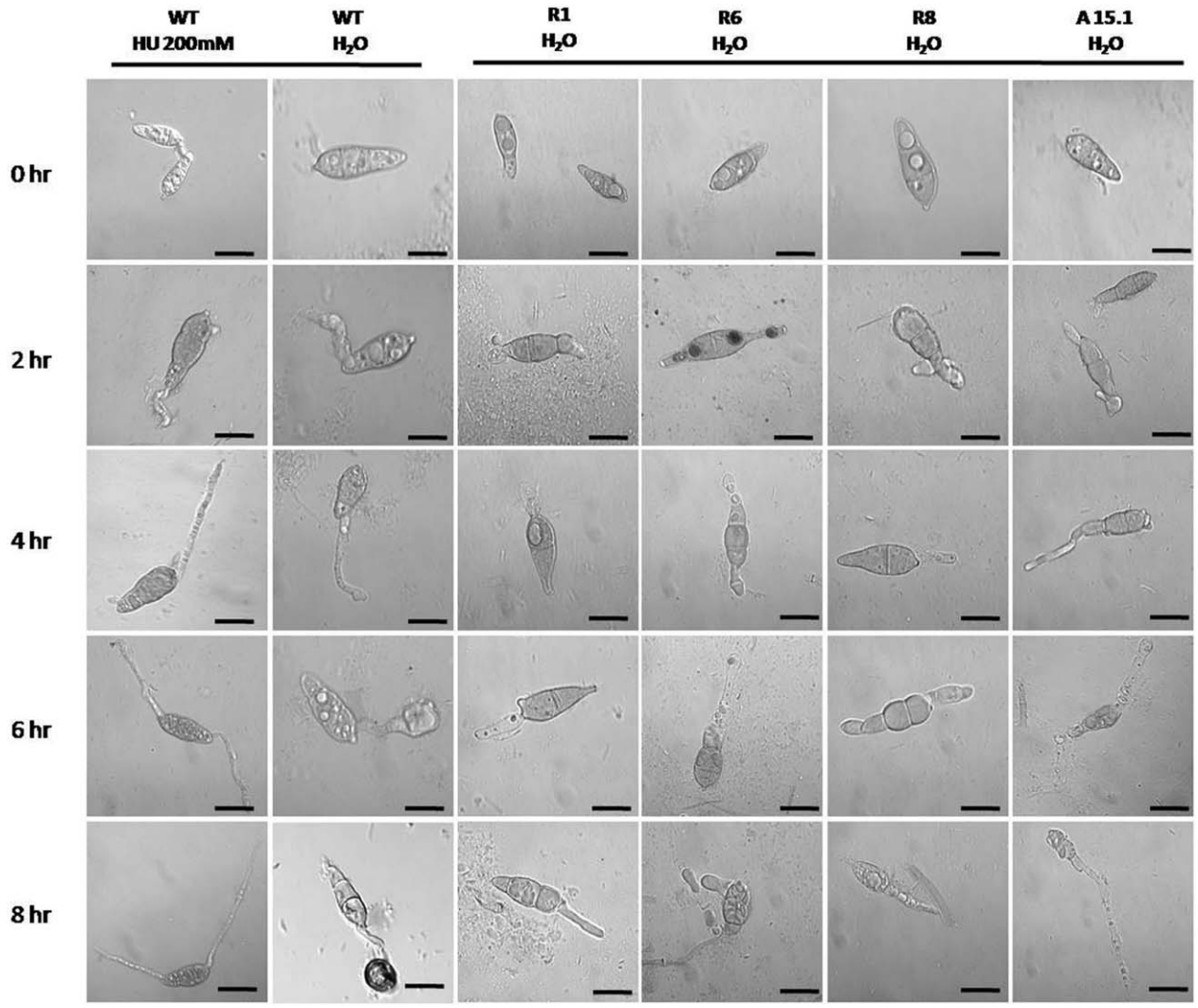

Fig. 8 *MoSKP1* RNA interference (RNAi) and antisense transformants are defective in the cell cycle. Wild-type *Magnaporthe oryzae* B157 strain was treated with hydroxyurea (200 mM) and checked for appressoria formation up to 8 h. Knockdown transformants and B157 were compared for appressorial development. B157 without hydroxyurea was taken as control. Bar, 10 μm.

orthologue of *Aspergillus nidulans nimO* and *S. cerevisiae* Dbf4p required for DNA replication (Jackson *et al.*, 1993; James *et al.*, 1999), suggest that S-phase entry is the regulatory commitment for appressorium maturation, whereas *bim1* mutations indicate that mitotic exit is required for infection. Bim1 is an orthologue of *A. nidulans* BimE and the *S. cerevisiae* APC large subunit, indicating that it may form a component of the *M. oryzae* APC, suggesting that proteolytic degradation is key to this regulation.

In *S. cerevisiae*, the Skp1 homologue Cbf3d, named so for its role as an important component of the CBF3-*CEN* complex, has been studied extensively (Stemmann and Lechner, 1996). This protein is essential for growth and for the execution of kinetochore function by interacting with cyclin A/CDK2 (Zhang *et al.*, 1995). It has been found that CLB1-4/CDC28 complexes or unidentified cyclin/CDK-like proteins might interact with Cbf3d directly or indirectly (Nasmyth, 1993).

In *Sc. pombe*, there are several F-box proteins, three of which [two essential (Pof1 and Pof3 involved in the maintenance of genome integrity) and one non-essential (Pof10)] are found to be involved in cell cycle regulation. The binding of Skp1 with these three F-box proteins was reduced in Skp1 temperature-sensitive mutant cells, as a result of which cells exhibited G2 delay, which is attributable to activation of the DNA damage check point. This implies a novel role for Skp1 in the checkpoint signalling cascade, in addition to that required for septum processing and cell separation in fission yeast (Hermand *et al.*, 2003; Lehmann and Toda, 2004).

Given the fact that ubiquitination controls cell cycle progression and development, we believe that our characterization of the

Skp1 homologue in *M. oryzae* B157 will facilitate the further investigation of the role of ubiquitination in growth and development in pathogenic fungi. MoSkp1 is predicted to be a 19.363-kDa protein with tetramerization and dimerization domains characteristic of its family. Various temperature-sensitive mutants have been generated for Skp1 in *Sc. pombe* and *S. cerevisiae*. We used the s*kp1 A7* mutant of *Sc. pombe* for interspecies gene complementation with MoSkp1. The wild-type phenotype of the fission yeast mutant s*kp1 A7* was largely restored in the complemented strain, although growth was slower and the size of cells was slightly smaller than in the wild-type, possibly because of the overexpression of the protein as a result of the high copy number of the vector. Phylogenetic analysis showed that MoSkp1 is closest to NcSkp1 of *N. crassa*. MoSkp1 is able to complement the function of *Sc. pombe* even though it is not very phylogenetically close. This indicates that, functionally, Skp1 is very much conserved, although we cannot rule out the possibility of other novel functions of *MoSKP1* apart from ubiquitination in *M. oryzae* B157.

The sequence analysis of MoSkp1 strongly suggests the presence of phosphorylation sites, together with its dimerization domain. Most of the potential phosphorylation sites of MoSkp1 were serine residues. Of five serine residues, those at positions 77, 81 and 83 are most likely to be phosphorylated, together with two threonine residues at positions 76 and 86, just in the vicinity of a serine residue. All the phosphorylation sites fall within a conserved stretch and participate in protein–protein interactions. The silencing efficiency in *MoSKP1* RNAi transformants was found to be higher when compared with the silencing in *MoSKP1* antisense transformants. The transcript levels of *MoSKP1* RNAi transformants varied from 15% to 40%, whereas, in *MoSKP1* antisense transformants, it increased to 60%. The decrease in *MoSKP1* transcript levels in the RNAi transformants leads to abnormal phenotypes in a manner consistent with the decrease in the level of transcripts, where transformants with the lowest transcript levels have minimum growth and sporulation, and transformants with intermediate transcript levels are able to grow and sporulate, but unable to form appressoria. These results suggest that the level of MoSkp1 is critical to its diverse functions. Although a transcript level of 40% appears to be sufficient for sporulation, much higher levels are required for appressorial development, and a further reduction to 20% leads to complete abolition of function. Mitosis is an important step in the development of appressoria and it is likely that Skp1 stabilizes the SCF E3 ubiquitin ligase complex, which plays an important role in cell cycle progression. The presence of MoSkp1 protein in spore, germ tube and appressoria when compared with mycelia provides strong evidence that MoSkp1 is necessary for the initial development of spores to appressoria, and thus for the development of the infection structure. Further, the silenced transformants behave similarly to the cell cycle-defective mutant *Sc. pombe skp1 A7*, and HU-treated *M. oryzae* also shows similar defects.

MoSkp1 interacts with MoFrp1, a hypothetical protein of *M. oryzae*, which is predicted to be an F-box protein in *M. oryzae* on the basis of homology and interaction studies in another pathogenic fungus *F. oxysporum*, where Frp1 is involved in pathogenesis. Yeast two-hybrid interaction investigation of MoSkp1 and MoFrp1 confirms the ability of these two proteins to interact and function in the protein complex. This opens up the possibility of the interaction of other F-box proteins with MoSkp1 to control various other processes in the cell.

Conclusion

In the light of previous information and our data, we were able to show that *M. oryzae* B157 Skp1 plays essential roles in the growth and development of the fungus and a crucial role in the morphogenesis of appressoria. It is evident from the data presented here that MoSkp1 is essential for the growth, sporulation, cell wall integrity, normal cellular physiology and development of infection structures.

EXPERIMENTAL PROCEDURES

Fungal strains, growth conditions and nucleic acid extraction

Magnaporthe oryzae isolate B157 was used in the present study (Kachroo *et al.*, 1994, 1995). The isolate was maintained and cultured on yeast extract glucose agar (YEG) medium. For sporulation, oat meal agar (OMA) was used. The s*kp1 A7* mutant of *Sc. pombe* was kindly provided by Professor Takashi Toda, Laboratory of Cell Regulation, London Research Institute, UK. Briefly, this strain is a temperature-sensitive mutant of s*kp1* in which the wild-type gene has been replaced by one-step gene replacement. CM for *M. oryzae* contained 0.1% yeast extract, 0.5% peptone, 0.1% tryptone, 1% glucose, and sodium nitrate 0.06% w/v, magnesium sulfate 0.05% w/v, potassium chloride 0.055% w/v and potassium dihydrogen phosphate 0.15% w/v as supplement. CM was used for the subculture of *M. oryzae*. Non-defined rich medium for *Sc. pombe* was yeast extract .2%, peptone 1%, dextrose 2% (YEPD) (Sambrook *et al.*, 1989). *Schizosaccharomyces pombe* was grown at 25 °C on Petri dishes. Transformants were grown on EMM phthalate (potassium hydrogen phthalate 0.3% w/v, sodium hydrogen phosphate 0.22% w/v, ammonium chloride 0.5%, D-glucose at 2% w/v, supplemented with salts, vitamins and minerals; pH was maintained at 6.5). Agar was added at 2% w/v to prepare solid medium. For both genomic DNA and total RNA extraction, the fungus was grown in 50 mL of YEG broth; a 3-day-old culture was harvested by filtering with Whatmann No. 1 filter paper, weighed, frozen in liquid nitrogen and ground with a pre-chilled mortar and pestle. The DNA was extracted following a standard protocol (Tendulkar *et al.*, 2003) with extraction buffer containing 0.1 M tris(hydroxymethyl)aminomethane (Tris) (pH 8), 0.05 M ethylenediaminetetraacetic acid (EDTA), 0.5% NaCl and 0.01% β-mercaptoethanol, followed by the precipitation by potassium acetate and

isopropanol, as described by Sambrook *et al.* (1989); TRIzol reagent (Invitrogen, CA, USA) was used for the extraction of RNA according to the manufacturer's instructions. The integrity of RNA was checked using non-denaturing gel electrophoresis and the concentration was estimated using a Nanodrop Spectrophotometer ND 1000 (Wilmington, DE, USA).

Identification of *MoSKP1* gene and generation of *MoSKP1* RNAi, antisense and overexpression transformants

The phytopathogenic fungus *F. oxysporum* s*kp1* gene was used as a query sequence in the TBLASTX search tool of NCBI to identify potential homologues in *M. oryzae*. A single hit was obtained from *M. oryzae* and other fungi. The highly conserved nucleotide sequence region was selected to design the primers (*Hind*III RSkp1F: 5′TTG**AAGCTT**ATGTCAGAGGG TCAGCTGCA3′) and (*Xho*I RSkp1R: 5′TTG**GAGCTC**ACGGTCCTCAGCCC ACTC3′) to amplify a 645-bp fragment of *MoSKP1* from *M. oryzae* B157 strain by PCR. This amplification product of *MoSKP1* was further used to make the RNAi construct. In order to create RNAi in *M. oryzae*, the pSilent Dual 2 vector (Nguyen *et al.*, 2008), a vector containing two constitutive TrpC promoters in opposite orientations flanking the multiple cloning site, was used. This plasmid contained hygromycin phosphotransferase (*hpt*) as a selectable marker. The gene fragment was amplified using XT-5 polymerase. The fragment was then cloned into the pSilent Dual 2 vector at *Hind*III and *Xba*I sites. Clones were confirmed by restriction digestion and PCR prior to fungal transformation. The new plasmid construct was named pSD2-*MoSKP1*.

In an alternative approach, an antisense construct was made using the pSilent vector (Nakayashiki, 2005; Nakayashiki and Nguyen, 2008). The primer sequences were designed in such a way that the amplification product had a *Kpn*I site at the 5′ and a *Bam*HI site at the 3′ end. After amplification, the PCR product was digested with *Kpn*I and *Bam*HI, and cloned at *Kpn*I and *Bgl*II sites (*Bam*HI and *Bgl*II have compatible ends) in the pSilent vector. Before fungal transformation, the construct was confirmed by restriction digestion and PCR. This construct was named pSilent-*MoSKP1*. An overexpression construct was generated by cloning the PCR product in the pSilent vector at the *Kpn*I and *Hind*III sites in the right orientation. The clone was confirmed by restriction digestion.

Magnaporthe oryzae isolate B157 was inoculated in 50 mL of YEG broth and grown for 3 days for each transformation experiment. Biomass was then filtered with Miracloth (Calbiochem, San Diego, CA, USA), washed with sterile distilled water and resuspended in 50 mL of sterile 1 M sorbitol containing 50 mg of lytic enzyme (Sigma, St. Louis, MO, USA). This was incubated overnight at 28 °C at 100 rpm for protoplasting. Protoplasts were filtered, washed and resuspended in 200 μL of STC buffer (1 M sorbitol, 50 mM Tris/HCl, pH 7.4, 50 mM calcium chloride) containing 5 μg of plasmid DNA. After 1 h of incubation at 28 °C, 1.2 mL of PTC [40% (w/v) polyethylene glycol 3550 (Sigma-Aldrich, Saint Louis, MO, USA), 50 mM Tris/chloride, pH 7.4, 50 mM calcium chloride] was added and the mixture was incubated for another 1 h at 28 °C under static conditions, before it was transferred to CMS (CM with 1 M sorbitol) for 16 h at 28 °C and 100 rpm. This suspension was mixed with top agar and plated on a selection plate containing 200 μg/mL hygromycin B. After three successive selections on hygromycin B, the presence of the transgene was confirmed by PCR. In Southern blot analysis, 10 μg of genomic DNA were digested with *Hind*III, and 0.8% agarose gel electrophoresis was performed to separate the digested products at 50 V for 8 h. After denaturation and neutralization of the digest in the gel, capillary blot transfer was performed for 16 h to transfer the DNA fragments onto a nylon membrane (Hybond N+, Amersham, Buckinghamshire, UK). The transferred DNA on the membrane was crosslinked by a UV crosslinker (Spectrolinker, XL-100, NY, USA) with a preset optimum cross-linking programme. A 350-bp fragment of the TrpC promoter of the vector was amplified and the probe was prepared according to the manufacturer's instructions (AlkPhos Labeling and Detection Kit, GE Healthcare, Little Chalfont, Buckinghamshire, UK).

Expression of MoSkp1, antibody generation, Western blot analysis and immunolocalization

Cloning of the 6 × His-*MoSKP1* fusion construct was performed by the initial amplification of cDNA of *MoSKP1* and subsequent cloning into pBluescriptKS$^+$ vector (Invitrogen). PCR was performed from cDNA template using a proofreading enzyme XT-5 polymerase (Bangalore Genei, Bangalore, India) and primers (forward primer: 5′CGAT**GAATTC**ATGTC AGAGGGTCAGCTGCA3′; reverse primer: 5′CGAT**GAGCTC**ACGGTCCTC AGCCCACTC3′) that introduced an *Eco*RI site at the 5′ end and an *Xho*I site at the 3′ end of the sequence. A 501-bp fragment (*MoSKP1* containing *Eco*RI and *Xho*I sites) derived from this vector was subcloned into pET30a vector (Novagen, Darmstadt, Germany). The recombinant 6 × His-MoSkp1 fusion protein was produced in *Escherichia coli* BL21 (DE3) and purified using an Ni-NTA column (Qiagen, Darmstadt, Germany), according to the manufacturer's guidelines. The concentration of the purified recombinant protein was estimated by the Bradford method (Bradford, 1976).

Polyclonal antibody was generated by immunizing a New Zealand White Rabbit using 100 μg of purified protein and an equal volume of Freund's complete adjuvant. Subsequently, two booster doses were given to the rabbit with Freund's incomplete adjuvant and, after 7 days, the rabbit was bled and antiserum was collected and checked for titre by enzyme-linked immunosorbent assay (ELISA) and Western blot. Western blot analysis was performed to detect the relative levels of MoSkp1 protein in the RNAi (R1, R2, R3, R6 and R8) and antisense (A6 and A15.1) transformants. Total protein was extracted from wild-type *M. oryzae* B157 strain and silenced transformants. The protein was estimated by the Bradford method and 20 μg of total protein were used for Western blotting. Sodium dodecylsulfate-polyacrylamide gel electrophoresis (12%) was run and transferred to a poly(vinylidene difluoride) (PVDF) membrane by the wet transfer method. Ponceau S staining was performed to confirm protein transfer and to check for equal loading of protein. The membrane was treated with 3% skimmed milk as a blocking agent and subsequently washed with phosphate-buffered saline pH 7.2, 0.1% Tween-20 (PBST). Rabbit polyclonal antibody against Skp1 was used as primary antibody and horseradish peroxidase (HRP)-conjugated anti-immunoglobulin G (IgG) against rabbit (Sigma) was used as secondary antibody. The bands were visualized by providing substrate 3,3′-diaminobenzidine (DAB) and hydrogen peroxide. A clear ~24-kDa band was detected in wild-type *M. oryzae*, and reduced levels of protein were detected in the transformants compared with the wild-type B157.

Anti-MoSkp1 antibody was used as primary antibody for the localization study in *M. oryzae* B157 strain. Spores, mycelia and developed

appressoria were fixed with fixing solution (formaldehyde, 10%; acetic acid, 5%; ethanol, 85%) for 1 h, followed by blocking solution bovine serum albumin (BSA 1%) and anti-MoSkp1 antibody treatment (Gupta and Chattoo, 2007). Anti-IgG against rabbit conjugated with TRITC (Sigma) was used as secondary antibody to detect the localized protein under 63× magnification with a motorized confocal laser microscope (Carl Zeiss, LSM 700, Oberkochen, Germany). Excitation of fluorescently labelled protein was performed at 557 nm with emission at 576 nm, and images were captured using a charged-coupled device camera (AxioCam HR, Jena, Germany), under the control of the Zen software package. Image analysis was performed with Zen software and Adobe Photoshop CS2.

Real-time PCR analysis for knockdown and overexpression transformants

Quantitative real-time PCR was performed on RNAi, antisense and overexpression transformants of *MoSKP1* in an ABI 7900 HT Fast Real Time PCR System (Applied Biosystems, CA, USA) by monitoring the increase in fluorescence of the SYBR Green dye in real time, according to the manufacturer's instructions. The primers (Skp1 real forward, 5′GTTCTTGAG TGGTGTGA3′; Skp1 real reverse, 5′GCATGAACTTCTGATCC3′; Mo Tubulin forward, 5′GAGTCCAACATCAACGATCT3′; Mo Tubulin reverse, 5′GTA CTCCTCTTCCTCCTCGT3′) for amplification were selected from the C-terminal end of the mRNA coding region, which amplifies 100 bp to ensure the detection of the remaining mRNA of the *MoSKP1* transcript. The PCR conditions were as follows: 10 min at 95 °C, followed by 40 cycles of 10 s at 95 °C, 10 s at 55 °C and 15 s at 72 °C. The relative quantification of target gene transcript in terms of fold change was calculated using the formula $2^{-\Delta\Delta Ct}$, where $\Delta\Delta Ct = (Ct_{\text{gene of interest}} - Ct_{\text{tubulin}})_{\text{test condition}} - (Ct_{\text{gene of interest}} - Ct_{\text{tubulin}})_{\text{control}}$. Each real-time PCR quantification was carried out in triplicate, and values for each gene were normalized to the expression level of the wild-type B157 and used further to calculate the ratio of the expression level of the transcript.

Expression of MoSkp1 in fission yeast mutant *skp1 A7*

Interspecies gene complementation was carried out by expressing the *M. oryzae* MoSkp1 in the s*kp1 A7* mutant of *Sc. pombe*. A vector was generated by subcloning cDNA of *MoSKP1* into yeast expression vector pYES2 under the inducible GAL1 promoter for complementation in yeast. PCR was performed to amplify a 501-bp DNA fragment using pBS/KS-cDNA *MoSKP1* as template and proofreading enzyme XT-5 polymerase (Bangalore Genei). The primers used were as follows: mRNA *Skp1 Xho*I For, 5′CGAT**GAGCTC**ATGTCAGAGGGTCAGCTGC3′; mRNA *Skp1 Xba*I Rev, 5′CGAT**TCTAGA**TTAACGGTCCTCAGCCCA3′. The PCR product was cloned into yeast expression vector pYES2 at *Xho*I and *Xba*I sites, and yeast transformation was performed by the lithium acetate method (Daniel and Wood, 2002). Putative transformants were selected on EMM medium containing 2% galactose, without uracil. The transformants were confirmed by PCR.

Plant pathogenicity test, onion epidermis assay, sporulation and appressorium development assay

Plant pathogenicity test was performed by allowing spores to infect rice leaves (CO39 rice cultivar). Spores from wild-type *M. oryzae* B157 strain, OES1 and *MoSKP1* RNAi transformants were harvested and the spore count was adjusted to 1×10^5 spores/mL; 50 μL of spore suspension were spotted onto the adaxial surface of a rice leaf and maintained at 24 °C in 90% humidity. The development of lesions was observed at 10 dpi, and the severity of infection was measured by counting the number of lesion spots per unit area of leaf.

Onion epidermis assay was performed to check the development of appressoria and further penetration of invasive hyphae. The spore count was maintained at 1×10^4 spores/mL and 50 μL of spore suspension were spread on a single layer of onion epidermis and kept in the dark for 12 h. The development of appressoria and the progression of the germ tube were observed under a microscope, and photographs were taken under a 100× oil immersion objective (Olympus BX51, Tokyo, Japan).

Appressorium development assay was performed by the application of spores to a hydrophobic surface. The spore count was maintained at 1×10^4 spores/mL and 20 μL of spore suspension were placed on a coverslip (Esco, Erie Scientific, Portsmouth, NH, US) for 12 h. The arrangement of conidia on conidiophores (Wang *et al*, 2013) and the development of appressoria were observed under a 100× oil objective (Olympus BX51) and 63× confocal LSM 700 (Carl Zeiss).

CFW and Hoechst staining

CFW (Sigma) was dissolved in Milli-Q water to make 1 mg/mL stock solution. A working solution was made by dilution in PBS to a final concentration of 10 μg/mL. After fixing, fungal mycelia and spore cells were incubated with PBS, 1% Triton X100 solution for 2 h, washed with PBS and stained for 10 min. Washing was performed to remove the remaining stain and the slide was mounted in 50% glycerol. Hoechst 33258 (Sigma) stock solution was prepared by dissolving 1 mg in 1 mL of Milli-Q water. A working solution was prepared by diluting in PBS to a final concentration of 2 μg/mL. Staining was performed for 5 min at room temperature.

ACKNOWLEDGEMENT

The authors would like to thank Professor Takashi Toda for supplying the *skp1 A7* mutant of *Schizosaccharomyces pombe*.

FUNDING

Financial support was provided by the University Grant Commission, New Delhi, India and by the Department of Biotechnology (DBT), Ministry of Science and Technology, Government of India. Award of J.C.Bose National fellowship to B.C. by the Department of Science and Technology, Government of India. The funders had no role in the study design, data collection and analysis, decision to publish or preparation of the manuscript.

REFERENCES

Adachi, K. and Hamer, J.E. (1998) Divergent cAMP signaling pathways regulate growth and pathogenesis in the rice blast fungus *Magnaporthe grisea*. *Plant Cell*, **10**, 1361–1374.

Angot, A., Peeters, N., Lechner, E., Vailleau, F., Baud, C., Gentzbittel, L., Sartorel, E., Genschik, P., Boucher C. and Genin, S. (2006) *Ralstonia solanacearum* requires F-box-like domain-containing type III effectors to promote disease on several host plants. *Proc. Natl. Acad. Sci. USA*, **103**, 14620–14625.

Ariza, R.R., Keyse, S.M., Moggs, J.G. and Wood, R.D. (1996) Reversible protein phosphorylation modulates nucleotide excision repair of damaged DNA by human cell extracts. *Nucleic Acids Res.* **24**, 433–440.

Bai, C., Sen, P., Hofmann, K., Ma, L., Goebl, M., Harper, J.W. and Elledge, S.J. (1996) SKP1 connects cell cycle regulators to the ubiquitin proteolysis machinery through a novel motif, the F-box. *Cell*, **86**, 263–274.

Bonman, J.M. (1992) Durable resistance to rice blast disease—environmental influences. *Euphytica*, **63**, 115–123.

Bonman, J.M., Sanchez, L.M. and Mackill, O. (1988) Effects of water deficit on rice blast. II. Disease development in field. *J. Plant Prot.* **5**, 67–73.

Brace, E.J., Parkinson, L.P. and Fuller, R.S. (2006) Skp1p regulates Soi3p/Rav1p association with endosomal membranes but is not required for vacuolar ATPase assembly. *Eukaryot. Cell*, **5**, 2104–2113.

Bradford, M.M. (1976) A rapid and sensitive method for the quantitation of microgram quantities of protein utilizing the principle of protein–dye binding. *Anal. Biochem.* **72**, 248–254.

Choi, W. and Dean, R.A. (1997) The adenylate cyclase gene MAC1 of *Magnaporthe grisea* controls appressorium formation and other aspects of growth and development. *Plant Cell*, **9**, 1973–1983.

Connelly, C. and Hieter, P. (1996) Budding yeast SKP1 encodes an evolutionarily conserved kinetochore protein required for cell cycle progression. *Cell*, **86**, 275–285.

Daniel, R.G. and Wood, R.A. (2002) Transformation of yeast by lithium acetate/single-stranded carrier DNA/polyethylene glycol method. *Methods Enzymol.* **350**, 87–96.

Duyvesteijn, R.G., van Wijk, R., Boer, Y., Rep, M., Cornelissen, B.J. and Harng, M.A. (2005) Frp1 is a *Fusarium oxysporum* F-box protein required for pathogenicity on tomato. *Mol. Microbiol.* **57**, 1051–1063.

Ebbole, D.J. (2007) *Magnaporthe* as a model for understanding host–pathogen interactions. *Annu. Rev. Phytopathol.* **45**, 437–456.

Feldman, R.M., Correll, C.C., Kaplan, K.B. and Deshaies, R.J. (1997) A complex of Cdc4p, Skp1p, and Cdc53p/cullin catalyzes ubiquitination of the phosphorylated CDK inhibitor Sic1p. *Cell*, **91**, 221–230.

Fourrey, V.C., Barooah, M., Egan, M., Wakley, G. and Talbot, N.J. (2006) Autophagic fungal cell death is necessary for infection by the rice blast fungus. *Science*, **312**, 580–583.

Gilbert, M.J., Thornton, C.R., Wakley, G.E. and Talbot, N.J. (2006) A P-type ATPase required for rice blast disease and induction of host resistance. *Nature*, **440**, 535–539.

Gupta, A. and Chattoo, B.B. (2007) A novel gene MGA1 is required for appressorium formation in *Magnaporthe grisea*. *Fungal Genet. Biol.* **44**, 1157–1169.

Hattori, T., Kitagawa, K., Uchida, C., Oda, T. and Kitagawa, M. (2003) Cks1 is degraded via the ubiquitin-proteasome pathway in a cell cycle-dependent manner. *Genes Cells*, **8**, 889–896.

He, M., Kershaw, M.J., Soanes, D.M., Xia, Y. and Talbot, N.J. (2012) Infection-associated nuclear degeneration in the rice blast fungus *Magnaporthe oryzae* requires non-selective macro-autophagy. *PLoS One*, **7**, e33270.

Hermand, D., Bamps, S., Tafforeau, L., Vandenhaute, J. and Makela, T.P. (2003) Skp1 and the F-box protein Pof6 are essential for cell separation in fission yeast. *J. Biol. Chem.* **278**, 9671–9677.

Jackson, A.L., Pahl, P.M.B., Harrison, K., Rosamond, J. and Sclafani, R.A. (1993) Cell cycle regulation of the yeast Cdc7 protein kinase by association with Dbf4 protein. *Mol. Cell. Biol.* **13**, 2899–2908.

James, S.W., Bullock, K.A., Gygax, S.E., Kraynack, B.A., Matura, R.A., MacLeod, J.A., McNeal, K.K., Prasauckas, K.A., Scacheri, P.C., Shenefiel, H.L., Tobin, H.M. and Wade, S.D. (1999) nimO, an *Aspergillus* gene related to budding yeast Dbf4, is required for DNA synthesis and mitotic checkpoint control. *J. Cell Sci.* **112**, 1313–1324.

Jones, D.T., Taylor, W.R. and Thornton, J.M. (1992) The rapid generation of mutation data matrices from protein sequences. *Comput. Appl. Biosci.* **8**, 275–282.

Kachroo, P., Leong, S.A. and Chattoo, B.B. (1994) Pot2, an inverted repeat transposon from the rice blast fungus *Magnaporthe grisea*. *Mol. Gen. Genet.* **245**, 339–348.

Kachroo, P., Leong, S.A. and Chattoo, B.B. (1995) Mg-SINE: a short interspersed nuclear element from the rice blast fungus, *Magnaporthe grisea*. *Proc. Natl. Acad. Sci. USA*, **92**, 11125–11129.

Kaplan, K.B., Hyman, A.A. and Sorger, P.K. (1997) Regulating the yeast kinetochore by ubiquitin-dependent degradation and Skp1p-mediated phosphorylation. *Cell*, **91**, 491–500.

Kim, N., Yoon, H., Lee, E. and Song, K. (2006) A new function of Skp1 in the mitotic exit of budding yeast *Saccharomyces cerevisiae*. *J. Microbiol. (Seoul, Korea)*, **44**, 641–648.

Koc, A., Wheeler, L.J., Mathews, C.K. and Merrill, G.F. (2004) Hydroxyurea arrests DNA replication by a mechanism that preserves basal dNTP pools. *J. Biol. Chem.* **279**, 223–230.

Lehmann, A. and Toda, T. (2004) Fission yeast Skp1 is required for spindle morphology and nuclear membrane segregation at anaphase. *FEBS Lett.* **566**, 77–82.

Lehmann, A., Katayama, S., Harrison, C., Dhut, S., Kitamura, K., McDonald, N. and Toda, T. (2004) Molecular interactions of fission yeast Skp1 and its role in the DNA damage checkpoint. *Genes Cells*, **9**, 367–382.

Murray, A.W. (2004) Recycling the cell cycle: cyclins revisited. *Cell*, **116**, 221–234.

Nakayashiki, H. (2005) RNA silencing in fungi: mechanisms and applications. *FEBS Lett.* **579**, 5950–5957.

Nakayashiki, H. and Nguyen, Q.B. (2008) RNA interference: roles in fungal biology. *Curr. Opin. Microbiol.* **11**, 494–502.

Nasmyth, K.F.C. (1993) Yeast G1 cyclins CLN1 and CLN2 and a GAP-like protein have a role in bud formation. *EMBO J.* **1**, 5277–5286.

Nguyen, Q.B., Kadotani, N., Kasahara, S., Tosa, Y., Mayama, S. and Nakayashiki, H. (2008) Systematic functional analysis of calcium-signalling proteins in the genome of the rice-blast fungus, *Magnaporthe oryzae*, using a high-throughput RNA-silencing system. *Mol. Microbiol.* **68**, 1348–1365.

Oh, Y., Franck, W.L., Han, S.O., Shows, A., Gokce, E., Muddiman, D.C. and Dean, R.A. (2012) Polyubiquitin is required for growth, development and pathogenicity in the rice blast fungus *Magnaporthe oryzae*. *PLoS One*, **7**, e42868.

Park, G., Xue, C., Zhao, X., Kim, Y., Orbach, M. and Xu, J.R. (2006) Multiple upstream signals converge on the adaptor protein Mst50 in *Magnaporthe grisea*. *Plant Cell*, **18**, 2822–2835.

Renski, L., Clijsters, L. and Wolthuis, R. (2008) To cell cycle, swing the APC/C. *Biochim. Biophys. Acta*, **1786**, 49–59.

Rosebrock, T.R., Zeng, L., Brady, J.J., Abramovitch, R.B., Xiao, F. and Martin, G.B. (2007) A bacterial E3 ubiquitin ligase targets a host protein kinase to disrupt plant immunity. *Nature*, **448**, 370–374.

Sambrook, J., Fritsch, E.F. and Maniatis, T. (1989) *Molecular Cloning: A Laboratory Manual, II*. New York: Cold Spring Harbor Laboratory Press.

Saunders, D.G.O., Aves, S.J. and Talbot, N.J. (2010a) Cell cycle-mediated regulation of plant infection by the rice blast fungus. *Plant Cell*, **22**, 497–507.

Saunders, D.G.O., Dagdas, Y.F. and Talbot, N.J. (2010b) Spatial uncoupling of mitosis and cytokinesis during appressorium-mediated plant infection by the rice blast fungus *Magnaporthe oryzae*. *Plant Cell*, **22**, 2417–2428.

Schulman, B.A., Carrano, A.C., Jeffrey, P.D., Bowen, Z., Kinnucan, E.R., Finnin M.S., Elledge, S.J., Harper, J.W., Pagano, M. and Pavletich, N.P. (2000) Insights into SCF ubiquitin ligases from the structure of the Skp1-Skp2 complex. *Nature*, **408**, 381–386.

Seol, J.H., Shevchenko, A. and Deshaies, R.J. (2001) Skp1 forms multiple protein complexes, including RAVE, a regulator of V-ATPase assembly. *Nat. Cell Biol.* **3**, 384–391.

Siino, J.S., Yau, P.M., Imai, B.S., Gatewood, J.M. and Morton, B.E. (2003) Effect of DNA length and H4 acetylation on the thermal stability of reconstituted nucleosome particles. *Biochem. Biophys. Res. Commun.* **302**, 885–891.

Singer, A.U., Schulze, S., Skarina, T., Xu, X., Cui, H., Eschen-Lippold, L., Egler, M., Srikumar, T., Raught, B., Lee, J., Scheel, D., Savchenko, A. and Bonas, U. (2013) A pathogen type III effector with a novel E3 ubiquitin ligase architecture. *PLoS Pathog* **9**(1): e1003121. doi: 10.1371/journal.ppat.1003121.

Singer, R.A. and Johnston, G.C. (1981) Nature of the G1 phase of the yeast S*accharomyces cerevisiae*. *Cell Biol.* **78**, 3030–3033.

Skamnioti, P. and Gurr, S.J. (2009) Against the grain: safeguarding rice from rice blast disease. *Trends Biotech.* **27**, 141–150.

Skowyra, D., Craig, K.L., Tyers, M., Elledge, S.J. and Harper, J.W. (1997) F-box proteins are receptors that recruit phosphorylated substrates to the SCF ubiquitin-ligase complex. *Cell*, **91**, 209–219.

Stemmann, O. and Lechner, J. (1996) The *Saccharomyces cerevisiae* kinetochore contains a cyclin-CDK complexing homologue, as identified by in vitro reconstitution. *EMBO J.* **15**, 3611–3620.

Talbot, N.J. (2003) On the trail of a cereal killer: exploring the biology of *Magnaporthe grisea*. *Annu. Rev. Microbiol* **57**, 177–202.

Tamura, K., Peterson, D., Peterson, N., Stecher, G., Nei, M. and K.S. (2011) MEGA5: molecular evolutionary genetics analysis using maximum likelihood, evolutionary distance, and maximum parsimony methods. *Mol. Biol. Evol.* **28**, 2731–2739.

Tendulkar, S.R., Gupta, A. and Chattoo, B.B. (2003) A simple protocol for isolation of fungal DNA. *Biotechnol. Lett.* **25**, 1941–1944.

Thakur, S., Jha, S., Barman, R.S. and Chattoo, B.B. (2009) Genomic resources of *Magnaporthe oryzae* (GROMO): a comprehensive and integrated database on rice blast fungus. *BMC Genomics*, **10**, 316.

Thines, E., Weber, R.W. and Talbot, N.J. (2000) MAP kinase and protein kinase A-dependent mobilization of triacylglycerol and glycogen during appressorium turgor generation by *Magnaporthe grisea*. *Plant Cell*, **12**, 1703–1718.

Vodermaier, H.C. (2004) APC/C and SCF: controlling each other and the cell cycle. *Curr. Biol.* **14**, R787–R796.

Wang, J., Du, Y., Zhang, H., Zhou, C., Qi, Z., Zheng, X., Wang, P. and Zhang, Z. (2013) The actin-regulating kinase homologue MoArk1 plays a pleiotropic function in *Magnaporthe oryzae*. *Mol. Plant Pathol.* **14**(5): 470–482.

Wang, Z.Y., Jenkinson, J.M., Holcombe, L.J., Soanes, D.M. and Fourrey, V.C. (2005) The molecular biology of appressorium turgor generation by the rice blast fungus *Magnaporthe grisea*. *Biochem. Soc. Trans.* **33**, 384–388.

Wilson, R.A. and Talbot, N.J. (2009) Under pressure: investigating the biology of plant infection by *Magnaporthe oryzae*. *Nat. Rev. Microbiol.* **7**, 185–195.

Xu, J.R. and Hamer, J.E. (1996) MAP kinase and cAMP signaling regulate infection structure formation and pathogenic growth in the rice blast fungus *Magnaporthe grisea*. *Genes Dev.* **10**, 2696–2706.

Yam, C.H., Ng, R.W., Siu, W.Y., Lau, A.W. and Poon, R.Y. (1999) Regulation of cyclin A-Cdk2 by SCF component Skp1 and F-box protein Skp2. *Mol. Cell. Biol.* **19**, 635–645.

Yu, H. (2007) Cdc20: a WD40 activator for a cell cycle degradation machine. *Mol. Cell*, **27**, 3–16.

Zhang, H., Kobayashi, R., Galaktionov, K. and Beach, D. (1995) p19Skp1 and p45Skp2 are essential elements of the cyclin A-CDK2 S phase kinase. *Cell*, **82**, 915–925.

Zhao, X. and Xu, J.R. (2007) A highly conserved MAPK-docking site in Mst7 is essential for Pmk1 activation in *Magnaporthe grisea*. *Mol. Microbiol.* **63**, 881–894.

Zhao, X., Kim, Y., Park, G. and Xu, J. (2005) A mitogen-activated protein kinase cascade regulating infection-related morphogenesis in *Magnaporthe grisea*. *Plant Cell*, **17**, 1317–1329.

Zhao, X., Mehrabi, R. and Xu, J.R. (2007) Mitogen-activated protein kinase pathways and fungal pathogenesis. *Eukaryot. Cell*, **6**, 1701–1714.

SUPPORTING INFORMATION

Additional Supporting Information may be found in the online version of this article at the publisher's website:

Fig. S1 Southern and western blot analysis of *MoSKP*1 RNA interference (RNAi) and antisense transformants. (a) Genomic DNA was digested with *Hind*III enzyme and the blot was probed with TrpC promoter (350 bp). Lanes 1–5 represent R1, R2, R3, R6 and R8 *MoSKP*1 RNAi transformants, respectively. pSD2-digested plasmid was loaded as positive control. (b) Genomic DNA isolated from *MoSKP*1 antisense transformants A15.1, A2, A3 and A6 was digested with *Xba*I. TrpC promoter was used as probe. (c) Total protein was isolated from *MoSKP*1 RNAi transformants and 20 μg of total protein was loaded in each lane. Protein levels were estimated using MoSkp1 antibody. (D) Protein levels of MoSkp1 in antisense transformants were analysed by western blot analysis by probing with the anti-MoSkp1 antibody. Equal loading of protein in each lane was confirmed by Ponceau S staining.

Fig. S2 Sporulation and transcript level expression of knockdown and overexpression transformants. Sporulation assay was performed on the eighth day after inoculation. The top panels show the sporulation assay with the *y*-axis being the spore count in 1 $\times$ 10^4/mL. The bottom panels show the respective transcript levels with the *y*-axis depicting the fold change for the respective transformants indicated on the *x*-axis. (a) Sporulation assay of *MoSKP*1 RNA interference (RNAi) transformants. (b) Sporulation assay of *MoSKP*1 antisense transformants. (c) Sporulation assay in OES1 and OES3. (d) Expression analysis of *MoSKP*1 RNAi transformants. (e) Expression analysis of *MoSKP*1 antisense transformants. (f) Expression analysis of OES1 and OES3.

Fig. S3 Abnormal conidiation and reduced appressoria formation in *MoSKP*1 RNA interference (RNAi) and antisense transformants. (a) Abnormal conidia formation was observed in *MoSKP*1 knockdown transformants. The percentages of conidia with double, single and no septum are represented along the *y*-axis. (b) Appressoria formation was checked for RNAi and antisense transformants on a hydrophobic surface. The relative percentages of ungerminated spores and spores that germinated to form a germ tube and appressoria were quantified. Experiments were performed in triplicate taking 100 spores in each case. (c) Representative photographs of appressorial assay for transformants after 12 and 36 h.

Fig. S4 *MoSKP*1 R6 RNA interference (RNAi) transformant showed decreased ubiquitination compared with wild-type B157 *Magnaporthe oryzae* strain. Total protein ubiquitination enrichment assay was performed by enriching ubiquitinylated protein and probed with anti-ubiquitin antibody. An equal amount of total protein was loaded in each lane and the first lane is the positive control (provided by Thermo Scientific Pierce, Rockford, IL, USA). Lane 'L' contains protein marker (97.4–14.4 kDa) (Bangalore Genei, Bangalore, India).

Fig. S5 MoSkp1 protein interacts with a putative F-box protein MoFrp1. (a) AH109 cells containing pGBKT7-MoSkp1, AH109 yeast cells containing pGADT7-MoFrp1 and AH109 yeast cells co-transformed with pGBKT7-MoSkp1 and pGADT7-MoFrp1 were spotted onto quadruple dropout medium; 20 μL of 1 : 10^6 and 1 : 10^7 dilutions were spotted for each transformant. (b) The presence of cloned vector (pGADT7-Frp1 and pGBKT7-Skp1) in AH109 yeast host strain was confirmed by western blot analysis. Total protein was isolated from AH109 yeast strain containing both constructs, and the presence of MoFrp1-HA protein was confirmed by anti-haemagglutinin (anti-HA) antibody and the presence of MoSkp1-Myc protein was confirmed by anti-Myc antibody. (c) Co-immunoprecipitation (Co-IP) of MoSkp1 and MoFrp1. Anti-Skp1 antibody was used to pull down MoSkp1 and MoFrp1 complex from total protein and purified using protein A resin. Lane 1 shows MoFrp1 detected by anti-HA antibody. Lane 2 shows co-immunoprecipitation using total protein of AH109 yeast cells without tagged proteins, and was unable to detect MoFrp1 protein.

Fig. S6 Real-time polymerase chain reaction (PCR) of *MoSKP1* in spore, germ tube and appressoria, and the quantification of blast lesions. (a) Real-time PCR of *MoSKP1* in spores, germ tubes (6 h after germination) and developed appressoria. The

fold change was calculated. Experiments were performed in triplicate. (b) The blast lesions were measured as percentage disease leaf area (% DLA) at 10 days post-inoculation (dpi). Experiments were performed in duplicate; data presented as ±standard error of the mean (SEM) from independent estimations.

List S1 Strains used in the development of the phylogenetic tree. Phylogenetic analysis of *Magnaporthe oryzae* (XP_359799.1), *Fusarium oxysporum* (AAT85970.1), *Neurospora crassa* (XP_959019.1), *Verticillium albo-atrum* (XP_003003165.1), *Gibberella zeae* (XP_387098.1), *Cordyceps militaris* (EGX94398.1), *Colletotrichum higginsianum* (CCF32791.1), *Nectriahae matococca* (XP_003052201.1), *Glarea lozoyensis* (EHL00027.1), *Glomerella graminicola* (EFQ24879.1), *Metarhizium acridum* (EFY90756.1), *Trichophyton rubrum* (XP_003230905.1), *Grosmannia clavigera* (EFW98759.1), *Pyrenophora tritici* (XP_001931415.1), *Rhizopus oryzae* (EIE77840.1), *Aspergillus oryzae* (XP_001817076.1), *Aspergillus clavatus* (XP_001273939.1), *Aspergillus kawachii* (GAA89882.1), *Aspergillus nidulans* (XP_659906.1), *Aspergillus fumigatus* (XP_754026.1), *Aspergillus niger* (EHA22420.1), *Schizosaccharomyces japonicas* (XP_002174379.1), *Ustilago maydis* (XP_760758.1), *Puccinia graminis* (XP_003335788.1), *Sclerotinia sclerotiorum* (XP_001598454.1), *Coniophora puteana* (EIW84951.1), *Piriformospora indica* (CCA69667.1), *Culex quinquefasciatus* (XP_001843442.1), *Candida orthopsilosis* (CCG21169.1) and *Schizosaccharomyces pombe* (NP_595455.1).